

Cyclization of acyl thiosemicarbazides led to new *Helicobacter pylori* α -carbonic anhydrase inhibitors

Arzu Gumus^{1,2}  | Ilaria D'Agostino^{2,3,4}  | Valentina Puca⁴  |
Valentina Crocetta⁴ | Simone Carradori⁴  | Luigi Cutarella⁵  | Mattia Mori⁵  |
Fabrizio Carta²  | Andrea Angeli²  | Clemente Capasso⁶  | Claudiu T. Supuran² 

¹Department of Chemistry, Faculty of Science and Art, Balikesir University, Balikesir, Turkey

²Department of Neurofarba, Section of Pharmaceutical and Nutraceutical Sciences, University of Florence, Florence, Italy

³Department of Pharmacy, University of Pisa, Pisa, Italy

⁴Department of Pharmacy, "G. d'Annunzio" University of Chieti-Pescara, Chieti, Italy

⁵Department of Biotechnology, Chemistry and Pharmacy, University of Siena, Siena, Italy

⁶Department of Biology, Agriculture and Food Sciences, National Research Council (CNR), Institute of Biosciences and Bioresources, Naples, Italy

Correspondence

Ilaria D'Agostino and Fabrizio Carta,
Department of Neurofarba, Section of
Pharmaceutical and Nutraceutical Sciences,
University of Florence, Via Ugo Schiff 6, 50019
Sesto Fiorentino, Florence, Italy.
Email: ilaria.dagostino@unifi.it and
fabrizio.carta@unifi.it

Funding information

TUBITAK (The Scientific and Technological
Research Council of Turkey); Italian Ministry
for University and Research (MIUR),
Grant/Award Number: FISR2019_04819; EU,
Grant/Award Number: PE00000007; COST
(European Cooperation in Science and
Technology), Grant/Award Number: CA21145

Abstract

The eradication of *Helicobacter pylori*, the etiologic agent of gastric ulcer and adenocarcinoma, is a big concern in clinics due to the increasing drug resistance phenomena and the limited number of efficacious treatment options. The exploitation of the *H. pylori* carbonic anhydrases (HpCAs) as promising pharmacological targets has been validated by the antibacterial activity of previously reported CA inhibitors due to the role of these enzymes in the bacterium survival in the gastric mucosa. The development of new HpCA inhibitors seems to be on the way to filling the existing antibiotics gap. Due to the recent evidence on the ability of the coumarin scaffold to inhibit microbial α -CAs, a large library of derivatives has been developed by means of a pH-regulated cyclization reaction of coumarin-bearing acyl thiosemicarbazide intermediates. The obtained 1,3,4-thiadiazoles (**10–18a,b**) and 1,2,4-triazole-3-thiones (**19–26a,b**) were found to strongly and selectively inhibit HpCA and computational studies were fundamental to gaining an understanding of the interaction networks governing the enzyme–inhibitor complex. Antibacterial evaluations on *H. pylori* ATCC 43504 highlighted some compounds that maintained potency on a resistant clinical isolate. Also, their combinations with metronidazole decreased both the minimal inhibitory concentration and minimal bactericidal concentration values of the antibiotic, with no synergistic effect.

KEYWORDS

acyl thiosemicarbazide, carbonic anhydrase, *Helicobacter pylori*, molecular docking, synergism

This is an open access article under the terms of the [Creative Commons Attribution](https://creativecommons.org/licenses/by/4.0/) License, which permits use, distribution and reproduction in any medium, provided the original work is properly cited.

© 2024 The Author(s). *Archiv der Pharmazie* published by Wiley-VCH GmbH on behalf of Deutsche Pharmazeutische Gesellschaft.

1 | INTRODUCTION

In the alarming scenario of the rise of bacterial-resistant phenotypes, surprising and encouraging data emerged from reports on *Helicobacter pylori* infections in the 2011–2022 period, highlighting a global decrease in the number of cases in adults.^[1] However, we are still waiting for statistics on the latest years that will be undoubtedly affected by the COVID-19 pandemic which slowed down the treatments of non-life-threatening diseases,^[2] caused a worrisome misuse of antibiotics and a large abuse of sanitizers and disinfectants,^[3,4] along with the disruption of data collection job.^[5,6] Evidence of the big concern around *H. pylori* infections has already been recorded in 2017 when the World Health Organization (WHO) ranked the microorganism in the list of high-priority bacteria.^[7] The urgent need for new antibacterials is clear^[8] and new chemical classes with innovative scaffolds and mechanisms of action, such as the inhibition of carbonic anhydrases (CAs, E.C. 4.2.1.1), have been recently proposed.^[9] CAs are ubiquitous metalloenzymes, mostly Zn²⁺-containing, reversibly hydrating carbon dioxide (CO₂) to bicarbonate ion (HCO₃⁻) and proton (H⁺), thereby involved in the regulation of several physiopathological pathways through pH homeostasis and CO₂ capture. Different enzymes belonging to the α , β , γ , and ι are CA classes reported to play crucial roles in bacterial species, being implicated in their survival, virulence, and pathogenicity. *H. pylori* encodes for two isoforms, the periplasmatic Hp α CA and the cytosolic Hp β CA, both involved in a dual enzyme system with urease (E.C. 3.5.1.5), acting as a buffering system to maintain a neutral cell pH and ensure the pathogen survival at the stomach pH (~2.0).^[10] HpCA isoenzymes have been fully characterized^[11–14] and several inhibitors reported to possess antibacterial activity in vitro and in vivo.^[15–19] Interestingly, coumarin derivatives have been proven to effectively inhibit bacterial α -CAs,^[20] likely acting with a prodrug suicide mechanism as described for human (h)CAs.^[21,22]

Traditional therapeutical options for *H. pylori* infection involve the use of two antibiotics, including clarithromycin, amoxicillin, metronidazole, or tetracycline, a proton pump inhibitor, and, in some cases, bismuth.^[23,24] However, different treatments are also used in clinics, such as the triple therapy with vonoprazan^[25] or levofloxacin and the reverse hybrid therapy, even if, generally, the empiric use of antibiotics regimens is often employed, resulting in both drug-resistance rising and gastro-intestinal microbiota dysbiosis.^[26,27] Apart from natural remedies and probiotics, not always so efficacious in eradicating the infection, the scientific community is putting efforts into the development of new chemical entities—thus obtained by rational design and (semi)synthesis—as anti-*H. pylori* drug candidates,^[9,28–32] especially with innovative mechanisms of action.

In this frame, the development of large derivatives libraries is preferred to fast explore the chemical space of the selected chemical scaffold and generate functional activity data. This is expected to allow the establishment of robust structure–activity relationships (SARs) and drive the following lead optimization process. Straightforward, few-step, and high-yielding synthetic pathways are undoubtedly favored in the project plan, especially those involving

organic reactions that afford products easily isolated with a high purity degree by filtration and/or recrystallization. In this context, several chemical moieties have been identified to possess high and specific reactivities, often regulated by the reaction conditions. Among them, acyl thiosemicarbazides offer the opportunity to react intramolecularly in a pH-dependent manner generating two different heteroaromatic cycles, thiadiazoles in an acid environment and triazolethiones at basic pH.^[33,34]

2 | RESULTS AND DISCUSSION

2.1 | Chemistry

2.1.1 | Rationale of the study

Aimed at developing a new library of anti-*H. pylori* agents acting by inhibiting the pathogen CA, we designed compounds endowed with an established CA-inhibiting chemotype, the coumarin nucleus (Figure 1).

In particular, the possibility of having access to a fast-obtaining series of coumarin-containing acyl thiosemicarbazides^[35,36] led us to better investigate the chemical space around the positions C6 and C7 of the 2*H*-chromen-2-one (coumarin) core by including different tails composed of two diverse heterocycles, the 1,3,4-thiadiazole and 1,2,4-triazole-3-thione rings. Thus, the acyl thiosemicarbazide intermediates (1–9a,b, Figure 1) were constructed by employing 6-hydroxycoumarin (a) and umbelliferon (b) (Figure 1) and then cyclized to furnish the desired products (10–26a-b, Figure 1).

In this context, the tails and the appendages on different positions on the coumarin chemotype have been recognized to play a central role in the generation of perspective CA inhibitors since they are reported to address the binding pose of the compounds into the enzyme catalytic pocket and their consequent isoform preference or selectivity, due to the establishment of specific interactions within the residues close to the active site. Moreover, the exploitation of HpCAs in the search for new pharmacological targets for antibacterial agents has recently emerged and to date, only a few compounds have been reported to strongly inhibit HpCAs.^[11,15–18] Therefore, the study of molecules endowed with a high degree of chemical diversity with respect to the previously reported ones could be helpful in collecting new data for a further rational design of inhibitors. In fact, the exploration of the interaction network that is generated and results in enzyme inhibition is highly auspicious. In this frame, the selection of these specific rings as coumarin appendages, that is, thiadiazoles and triazolethiones, could represent an effective tool to further validate our computational models and gain a deeper insight into the enzyme–inhibitor complexes, being unprecedentedly investigated in CA inhibitors. Furthermore, the straightforward synthetic approach employed provided the opportunity to elucidate the impact of a simple substitution on the phenyl rings of the thiadiazole and triazolethione appendages on the affinity to the targeted enzyme. This could be easily achieved by comparing the kinetic activities and the binding poses of the compounds.

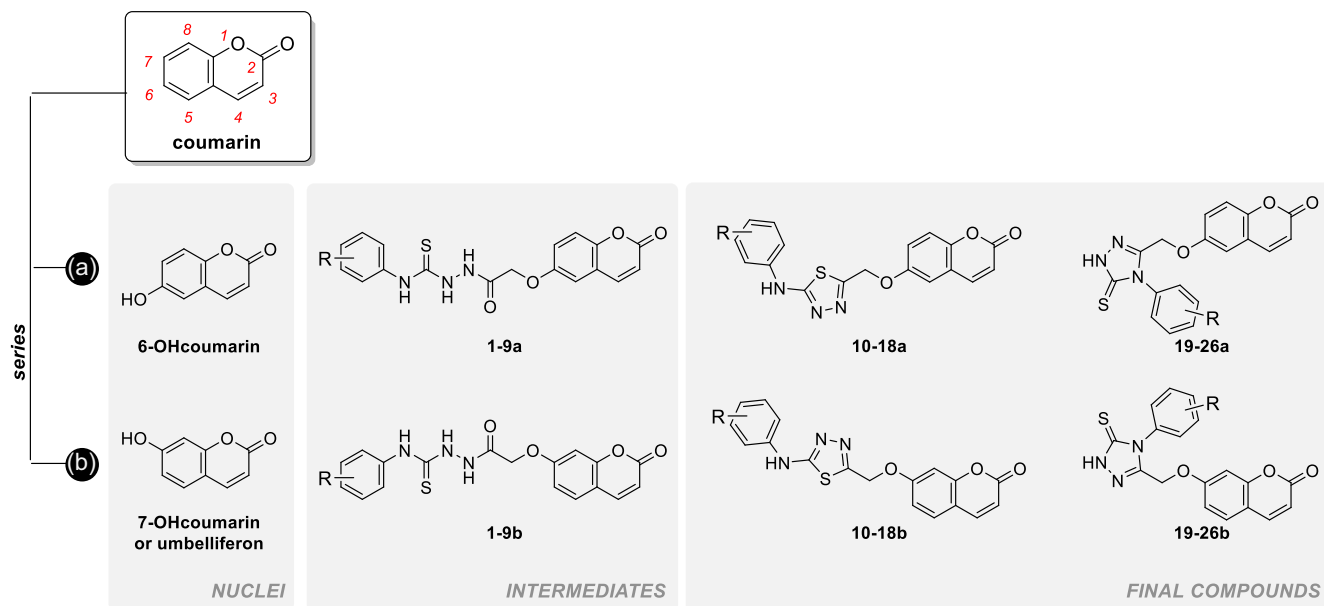


FIGURE 1 Structure of coumarin and the two series of compounds described in this work, **a** and **b**, with the nuclei, intermediates, and final compounds.

2.1.2 | Synthesis of the compound libraries

Acyl thiosemicarbazide-substituted coumarins **1–9a,b** were obtained in a four-step synthetic pathway starting from the suitable hydroxycoumarins **a–b**, as previously reported by us (Supporting Information S1: Figure S1).^[35,36] Then, derivatives **1–9a,b** underwent different cyclization reactions. Treatment with concentrated sulfuric acid gave 1,3,4-thiadiazoles **10–18a,b**, while in aqueous basic alkali, 1,2,4-triazole-3-thiones **19–26a,b** were obtained, as depicted in Scheme 1.

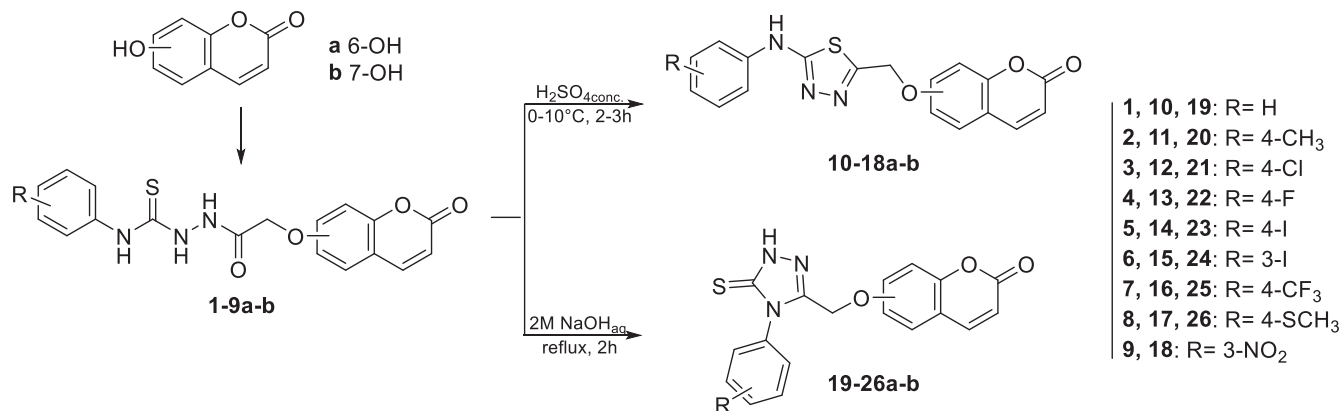
2.2 | In vitro inhibition of and preliminary SAR considerations

The inhibition profile for thiadiazoles **10–18a–b** and triazolethiones **19–26a–b** and the reference acetazolamide (AAZ) was assessed on a large panel of CAs from different microorganisms, including Gram-negative bacterial pathogens—*H. pylori* (HpCA),^[11] *Vibrio cholerae* (VchCA),^[37] and *Neisseria gonorrhoeae* (NgaCA)^[38]—hermophilic bacteria—*Sulfurihydrogenibium azorense* (SazaCA)^[39] and *Sulfurihydrogenibium yellowstonense* (SspaCA)^[40] protozoa—*Trypanosoma cruzi* (TcaCA)^[41] and *Plasmodium falciparum* (PfnCA)^[42]—parasites—*Schistosoma mansoni* (SmaCA),^[43] through the stopped-flow CO₂ hydration assay,^[44] and to evaluate selectivity, the physiologically relevant hCAs I and II were also tested. The results for the thiadiazole series are reported in Table 1 as inhibition constants (K_i values).

Observing Table 1, the whole set of thiadiazoles **10–18a,b** showed a lack of activity towards hCA I and II, even if, in sporadic cases, a moderate micromolar inhibition can be noticed. As regards

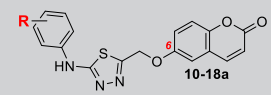
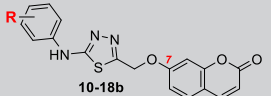
HpaCA (Table 1), the unsubstituted phenyl ring (R=H) is better tolerated when the *O*-substitution is in C6 (**10a**) with a decreased K_i value compared to the C7 isomer (**10b**). Otherwise, the introduction of an electron-donor substituent in *para*-position, such as the methyl group of **11a,b**, reversed the inhibitory activity, with the C7 isomer (**11b**) possessing a sixfold lower K_i than that of **11a**. The coumarin substitution position does not seem to significantly affect the activity when electron-withdrawing substituents, such as chlorine and fluorine atoms in **12–13a,b**, are introduced in the compound structure. However, the presence of the larger atom of iodine in the series **14–15a,b** caused an increase in K_i values, except for compound **14a** with the halogen present in *para*-position and the coumarin substitution pattern in C6. The trifluoromethyl group of the compounds couple **16a,b** was found to not alter the inhibition of the HpaCA isoform compared to the phenyl unsubstituted in **10a,b**. Remarkably, thiomethyl function is responsible for the highest potency in the series, with no differences between the coumarin isomers **17a,b**. Nitro group in *meta*-position in derivatives **18a,b** positively affects the inhibitory profile of the thiadiazole scaffold, with low nanomolar activities.

On the other hand, a broader activity variability was detected for VchCA (Table 1). Medium-high nanomolar inhibition was found for the unsubstituted derivatives **10a,b**, and a similar low potency emerged for the pattern with tolyl moiety and the coumarin functionalization in C6 (**11a**). Instead, its C7-isomer, compound **11b**, showed a relevant decrease in K_i value. Among the halo-derivatives **12–15a,b**, the *meta*-fluorophenyl group and the C6 *O*-substitution (**13a**) are the best patterns for inhibitory activity, resulting in a K_i value comparable to that of the reference AAZ. Worthy of interest are also both the coumarin isomers with the *meta*-iodophenyl ring (**15a,b**). Surprisingly, **13a** emerged also as a potent inhibitor of



SCHEME 1 Synthesis of coumarin derivatives **10-26a,b**.

TABLE 1 Inhibition data of thiadiazoles **10-18a,b** and reference compound AAZ on a panel of human (h) and nonhuman CA isoforms through the stopped-flow CO₂ hydration assay.^[44]

CPD	O-sub	R	K _i (nM) ^a									
			hCA I	hCA II	HpaCA	VchaCA	NgαCA	SspaCA	SazaCA	TcaCA	SmaCA	PfηCA
	6	H	n.a.	54,535	61.9	317	60.0	47.2	3615	87.5	24.7	146
	7	H	n.a.	n.a.	156	674	94.2	70.7	53.2	90.9	30.0	121
	6	4-CH ₃	n.a.	n.a.	63.7	475	72.0	64.2	3005	91.4	58.0	79.9
	7	4-CH ₃	n.a.	n.a.	5.7	64.0	16.0	79.1	299	586	33.6	158
	6	4-Cl	90,339	37,739	55.2	46.0	284	72.2	312	520	238	35.6
	7	4-Cl	n.a.	n.a.	37.6	43.8	59.3	92.2	279	1058	50.4	300
	6	4-F	91,662	24,385	43.2	10.0	10.0	10.0	245	120	6.3	14.2
	7	4-F	34,376	96,780	34.7	72.4	51.5	64.2	1235	367	29.8	184
	6	4-I	n.a.	n.a.	5.9	56.3	55.6	71.7	137	127	30.3	289
	7	4-I	n.a.	79,918	132	52.8	67.1	85.0	32.6	1029	49.4	71.4
	6	3-I	45,198	26,675	172	18.0	20.2	87.5	229	117	23.9	63.3
	7	3-I	33,314	33,219	35.6	16.9	22.8	79.5	313	101	39.5	185
	6	4-CF ₃	n.a.	30,343	48.0	72.6	34.4	58.0	2133	120	50.7	81.1
	7	4-CF ₃	n.a.	96,524	53.2	28.3	50.9	40.0	318	85.5	24.2	27.4
	6	4-SCH ₃	n.a.	40,187	5.2	56.4	74.8	82.2	300	78.1	48.0	23.0
	7	4-SCH ₃	n.a.	71,197	5.5	64.7	81.1	67.1	280	111	23.1	32.0
	6	3-NO ₂	n.a.	25,260	26.2	54.7	67.8	70.8	229	108	30.2	208
	7	3-NO ₂	n.a.	8735	35.5	58.3	33.7	69.4	238	125	48.2	1013
AAZ			250	12.1	21.4	6.8	75.0	4.5	0.90	61.6	42.5	170

Note: Errors are in the range of ±5%–10% of the reported values. n.a.: not active at 100 μM.

^aK_i values are reported as means of three independent experiments by a stopped-flow technique.

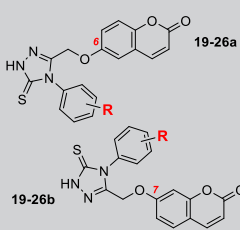
NgaCA and SppCAa (Table 1). SazCA was proved to be the less inhibited isoenzyme, with the whole library of thiazazole exerting from a moderate-high nanomolar to a low micromolar inhibitory activity (Table 1). On this trend, a few exceptions can be highlighted, that is, **10b** and **14b** show low nanomolar K_i values. Interestingly, data on protozoan CA from *T. cruzi* cover a wider K_i set of concentrations, with higher potency for some derivatives, such as the unsubstituted **10a-b** and slight micromolar inhibition by **11a**, **13b**, and **14b** (Table 1). Otherwise, similar K_i values were assessed against SmaCA, not consenting to perform any robust SARs, even if *para*-fluorophenyl derivative **13a** was the best-in-class compound against this isoenzyme in terms of activity, with a K_i lower than that of AAZ (Table 1). In the end, the η -enzyme from *P. falciparum* resulted more inhibited by compounds in which methyl (**11a**), chloro (**12a**), and fluoro (**13a**) substitution in *para*-position is combined to the C6 coumarin-functionalization than their corresponding isomers **11-13b** (Table 1). The same observation can be done for *meta*-iodo (**15a**) and

meta-nitro (**18a,b**) derivatives, while the trend is reversed for compounds **14a,b** and **16a,b** and no difference was found for **10a,b** and **17a,b** pairs.

Table 2 contains the K_i values for the triazolethione series.

As for the other compounds, triazolethiones were all found inactive towards hCAs, while large variability in inhibiting HpaCA was highlighted (Table 2). In particular, when the phenyl ring was left unsubstituted, a difference in activity was observed for the C6 (**19a**) and C7 (**19b**) coumarin isomers, with the latter showing more than 100 times smaller K_i values (Table 2). This feature could be noticed also for the other bacterial pathogens *V. cholerae* and *N. gonorrhoeae*. A specific trend of substitution and isomerism cannot be determined for the other derivatives; however, some compounds emerged for their low-nanomolar range of activity against HpaCA, that is, **20b** and **24a**. On the other hand, these two compounds lose their potency on VchaCA and NgaCA, reaching sometimes micromolar K_i values. Against SspaCA, the whole set of compounds seems to produce the

TABLE 2 Inhibition data of triazolethiones **19-26a,b** and reference compound AAZ on a panel of human (h) and nonhuman CA isoforms through the stopped-flow CO₂ hydration assay.^[44]



CPD	O-sub.	R	K_i (nM) ^a									
			hCA I	hCA II	HpaCA	VchaCA	NgaCA	SspaCA	SazaCA	TcaCA	SmaCA	Pf η CA
19a	6	H	n.a.	n.a.	297	945	2970	88.9	70.9	67.5	3169	237
19b	7	H	n.a.	n.a.	20.3	92.2	873	75.1	26.1	89.0	3455	28.7
20a	6	4-CH ₃	n.a.	n.a.	9.3	590	3962	49.6	3285	584	8846	285
20b	7	4-CH ₃	n.a.	n.a.	57.0	396	842	50.0	380	73.0	8339	819
21a	6	4-Cl	n.a.	n.a.	66.3	64.9	392	89.5	143	120	5299	93.8
21b	7	4-Cl	n.a.	n.a.	86.4	91.8	908	68.9	23.3	590	6677	25.4
22a	6	4-F	n.a.	n.a.	73.3	59.6	582	70.6	159	99.7	>10,000	88.4
22b	7	4-F	n.a.	n.a.	63.0	300	734	67.6	157	119	4414	30.6
23a	6	4-I	n.a.	n.a.	263	61.0	4464	76.9	30.1	94.2	756	28.1
23b	7	4-I	n.a.	n.a.	67.6	77.0	1793	74.8	33.5	110	832	31.9
24a	6	3-I	n.a.	31524	9.8	76.1	368	85.0	235	24,250	>10,000	591
24b	7	3-I	n.a.	n.a.	93.7	175	5296	78.5	221	104	>10,000	246
25a	6	4-CF ₃	n.a.	n.a.	342	75.2	95.1	75.0	90.2	128	4409	32.0
25b	7	4-CF ₃	n.a.	n.a.	34.5	69.1	6481	81.6	28.8	111	8189	179
26a	6	4-SCH ₃	n.a.	n.a.	74.4	54.6	94.0	73.7	29.2	342	649	15.7
26b	7	4-SCH ₃	n.a.	n.a.	322	53.4	307	16.9	13.9	120	76.9	31.2
AAZ			250	12.1	21.4	6.8	75.0	4.5	0.90	61.6	42.5	170

Note: Errors are in the range of $\pm 5\%$ – 10% of the reported values. n.a.: not active at 100 μM .

^a K_i values are reported as means of three independent experiments by a stopped-flow technique.

same effect, all reporting comparable K_i for a slight improvement in terms of potency for the mercaptomethyl phenyl derivative **26b** (Table 2). Small chemical differences corresponded to a jump in the activity profile of the compounds toward the SazαCA isoform and this is the open-and-shut case of tolyl derivatives **20a,b** and less evident for 4-chlorophenyl **21a,b** (Table 2). Moreover, also on this isoform, **26b** represents the best-in-class derivative in terms of inhibitory profile. TcaCA, instead, resulted in being less susceptible to this series of compounds and the substitution of the phenyl ring with different groups worsened the inhibitory activity from medium-low (**19a,b**) to moderate nanomolar range (Table 2). Also, the compounds are not well tolerated by the parasitic *S. mansoni* enzyme, resulting in a micromolar inhibitory potency or complete inactivity (Table 2). 7-Coumarins with the unsubstituted phenyl ring (**19b**) or bearing halogen atoms (chlorine in **21b** and fluorine in **22b**) turned out to possess a higher potency with respect to their corresponding isomers (**19a**, **21a**, and **22a**) against PflCA (Table 2). Moreover, the isomerism does not significantly affect the activity profile when the *para*-iodo (**23a,b**) and mercaptomethyl (**26a,b**) groups are introduced to the compound. Interestingly, most of the compounds were found to possess high selectivity for HpaCA over the other CAs from pathogens (NgaCA, TcaCA, SmaCA, and PflCA), as emerged by calculated selectivity indexes (SIs), reported in the heat map in Supporting Information S1: Figure S2. Interestingly, the whole library of compounds (**10–26a,b**) possesses a more potent bacterial CA-inhibiting profile with respect to the 6- and 7-hydroxycoumarins **a–b** which showed K_i values in the low micromolar range (92–77 and 77–68 μM on NgaCA and VchaCA, respectively).^[20] Remarkably, it is the first time a coumarin-based library is reported for its HpaCA inhibitory activity, and although the potency of such derivatives is significantly lower than that of previously reported sulfonamide-containing compounds (endowed with K_i values ranging from the sub-nanomolar to the high nanomolar concentrations).^[9,43,45–47] Indeed, the coumarin core has a positive gain in isoform selectivity, being (almost) inactive against physiologically relevant hCAs I and II, avoiding the risk of off-target effects.

2.3 | In silico studies on HpaCA

To rationalize the enzymatic assay results, representative compounds of the thiadiazole and triazolethione series were selected for an in silico investigation of the key interactions with HpaCA. In particular, molecular docking simulations were performed on triazolethione derivatives **20**, **24**, and **25**, which showed strong inhibition of HpaCA, with one of the isomers being significantly more potent than the other, as well as on the thiadiazole **17** that showed the strongest HpaCA inhibition with no discrepancy among isomers.

The crystallographic structure of the HpaCA isoform available in the Protein Data Bank (PDB ID: 4XFW),^[48] was used as a rigid receptor in docking simulations. Selected compounds were sketched in 2D format with the coumarin ring in its closed (intact coumarin core) and open (corresponding cinnamic acid derivatives in both *E* and *Z*

alkene geometries) conformation, the latter resulting from the hydrolysis mediated by the CA Zn(II)-coordinated hydroxide ion/water.^[49] A water molecule was manually added to the HpaCA structure in a geometry that corresponds to Zn(II) coordination, in agreement with previous works.^[50–52] Based on the proposed mechanisms of CA-mediated coumarin hydrolysis,^[21,50] only the closed conformation of the molecules was docked in the presence of the Zn-coordinated water molecule, whereas *E/Z* open derivatives were docked directly to the water-free form of the catalytic Zn(II) ion. Docking results were analyzed for pairs of isomers in both closed and *E/Z*-configured open forms, and considering the molecules as composed of three portions: (i) a coumarin/cinnamic head, (ii) a central portion consisting of a heterocyclic ring (thiadiazole or triazolethione), and (iii) a tail aromatic portion.

Triazolethione derivatives **20**, **24**, and **25** notably bind in a similar pose independently from the chemical nature and position of the substituent in the tail portion (Figure 2). In their closed form (Figure 2, left panels), the coumarin ring of these molecules binds the Zn-coordinated water molecule with an overlapping geometry. The difference between the two isomers **a** and **b** stands in the docking position of the central triazolethione, and, consequently, of the tail moiety. In **20a**, **24a**, and **25a**, the triazolethione group is T-shaped to the side chain of Phe42, whereas this interaction is not established by the respective **b** isomers. The tail portion of the **a** isomers is docked in a hydrophobic region bounded by Phe42 and Pro194, while the aromatic tail of the **b** series is docked in a more polar region surrounded by Lys133, Leu139, and Thr196, which might explain why hydrophobic contributions are privileged in **20a** and **24a** compared to the corresponding **b** isomers, whereas polar moieties are endowed with a stronger affinity such as in **25b** compared to **25a**.

By analyzing the open *Z*-configured conformations (Figure 2, middle panels), isomers assume rather different poses with respect to the coordination of the catalytic Zn(II) ion. Consistent with the mechanism of coumarin hydrolysis, **20a** and **24a** adopt a more suitable docking pose than the corresponding **b** isomers within the catalytic Zn(II) ion, given that the phenolic OH cooperates with the carboxylic ion in zinc coordination. This pose is also shared by both **25a** and **25b**, which might corroborate the stronger HpaCA inhibitory activity of the **a** isomer and **25b**. Finally, **20a**, **24a**, **25a**, and **25b** establish a parallel-displaced pi-stacking interaction with His84.

The carboxylic ion of open *E*-configured derivatives **20**, **24**, and **25** (Figure 2, right panels) shows a highly similar binding mode to the catalytic Zn(II) ion, with the phenolic OH being engaged in a H bond with Lys88 side chain. In **20b**, **24b**, and **25b**, the triazolethione ring is T-shaped with Phe42, while the aromatic tail portion is embedded in a hydrophobic region bounded by Phe42 and Pro194 that corresponds to the docking site of the tail of the **a** isomers in their closed coumarin form (Figure 2, left panels). In contrast, the triazolethione of **20a**, **24a**, and **25a** is docked in proximity to Pro194, while the aromatic ring of the tail portion is T-shaped with the side chain of Phe42. While for compounds **20** and **24**, molecular docking suggests some

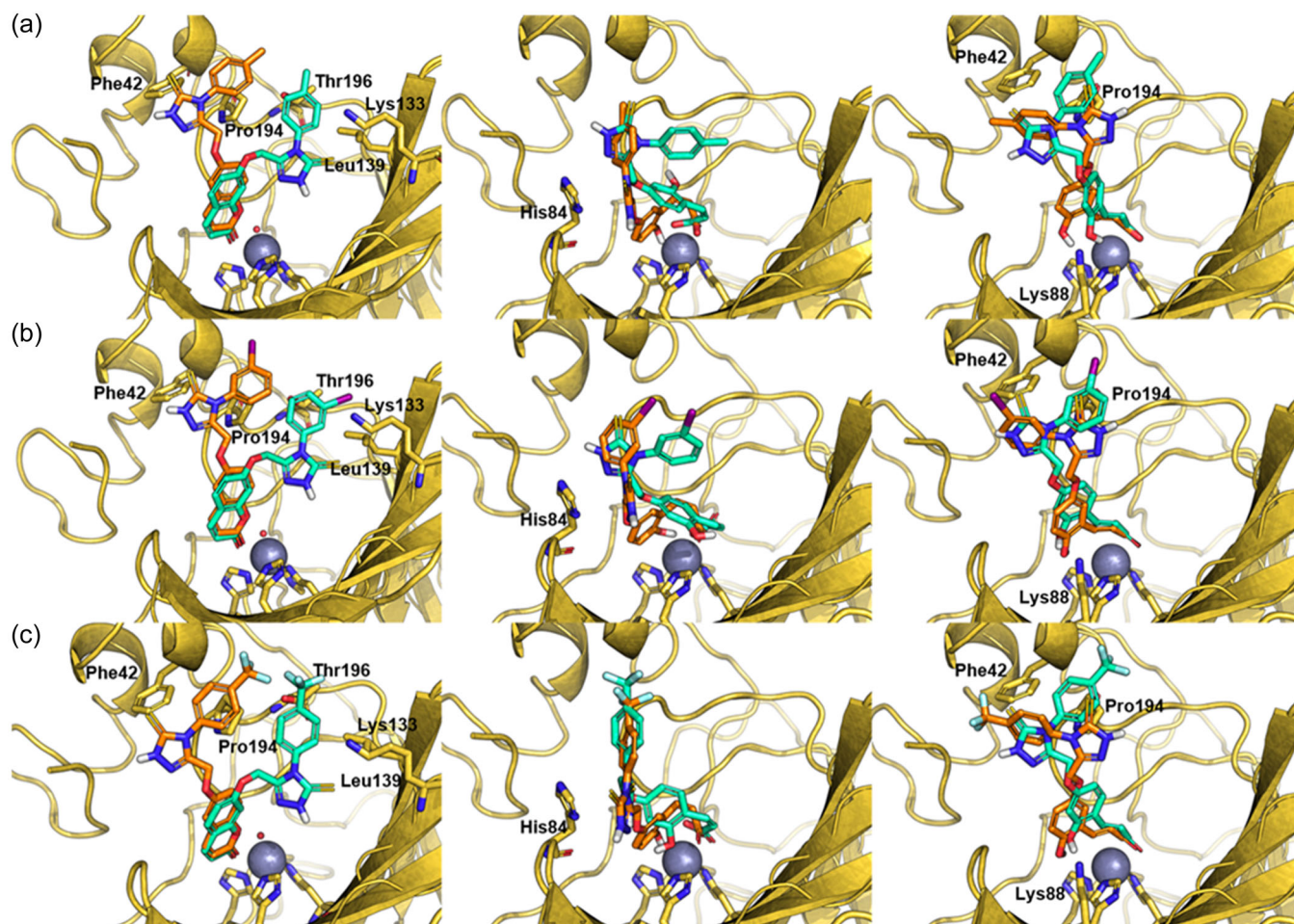


FIGURE 2 Predicted binding mode of **20** (a), **24** (b), and **25** (c) in the three forms investigated by molecular docking simulations: the closed coumarin form is shown in the left panel, the open *Z*-configured cinnamic acid form is shown in the middle panel, and the open *E*-configured cinnamic acid form is shown in the right panel. Compounds **20a**, **24a**, and **25a** are shown as orange sticks. Compounds **20b**, **24b**, and **25b** are shown as green sticks. The crystallographic structure of HpaCA is shown as a yellow cartoon, residues involved in binding to the molecules studied in this work, and described in the text, are shown as sticks and are labeled. The catalytic Zn(II) ion is shown as a gray sphere and the Zn-coordinated water molecule is shown as a small red sphere.

structural features that might rationalize the different HpaCA inhibition profile, this is not immediately true for **25**, suggesting that the effective contribution of the trifluoromethyl group might not be accounted for in molecular docking simulations.

In the case of the thiaziazole derivative **17**, it is interesting to note that subtle differences in the main scaffold compared to triazolethiones described above are reflected in different docking poses. In the closed coumarin form, the coumarin ring of both compounds interacts with the Zn(II)-coordinated water with different orientations. In the central part of the molecules, the thiaziazole group of **17a** is in proximity to Pro194 as well as it is T-shaped with the side chain of Phe42. Differently, the thiaziazole of **17b** establishes an H-bond interaction with Lys133, whereas the hydrophobic tail of both molecules converges to the same binding spot in proximity to Pro194. Docking poses of the open *Z*-configured cinnamic acid form (Figure 3, middle panel) show slight differences only within Zn(II)-coordination. While the cinnamic acid moiety of both **17a** and **17b** is

coordinated to the catalytic Zn(II) ion, the phenolic group of **17a** still participates in Zn(II) coordination, whereas in **17b** it is H-bonded to Asn108. The thiaziazole group of **17a** and **17b** is stacked over the side chain of His84, although with a different conformation (i.e., parallel-displaced and T-shaped, respectively) while the hydrophobic tail is docked in a non-polar region. Finally, the open *E*-configured cinnamic acid forms of **17** bind in a highly superimposable pose (Figure 3, right panel). Overall, in the three forms, the pharmacophores of **17a** and **17b** are generally well overlapped by docking simulations, which might rationalize the similar potency of these two molecules as observed in HpaCA inhibition.

2.4 | Anti-*H. pylori* bacterial susceptibility testing

Selected coumarin compounds were tested on two *H. pylori* strains, the reference ATCC 43504 and F1 clinical isolate, based on their

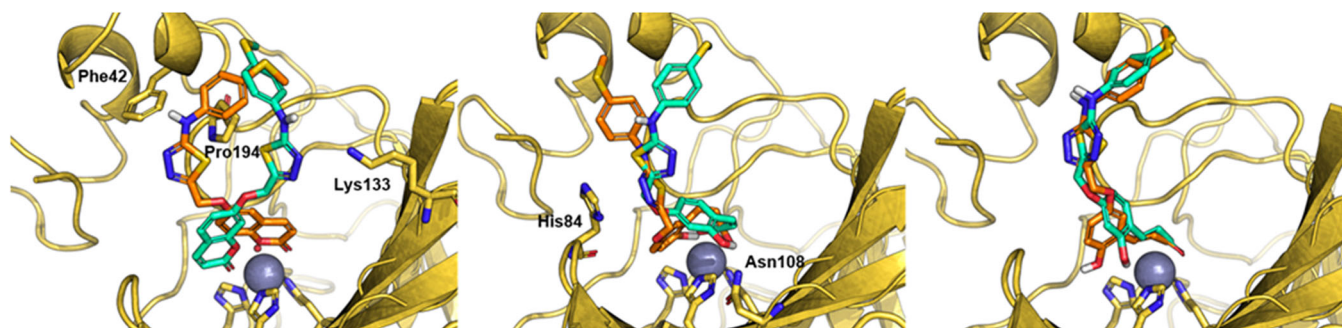


FIGURE 3 Predicted binding mode of compounds **17a** (orange sticks) and **17b** (green sticks) in the closed conformation (left panel), open Z-configured conformation (middle panel), and open E-configured conformation (right panel). The crystallographic structure of HpaCA is shown as a yellow cartoon, residues involved in binding to the molecules studied in this work, and described in the text, are shown as sticks and are labeled. The catalytic Zn(II) ion is shown as a gray sphere and the Zn(II)-coordinated water molecule is shown as a small red sphere.

different susceptibility profiles: the former is resistant to metronidazole (MTZ), while the latter is susceptible to amoxicillin (AMX) and MTZ but resistant to clarithromycin (CLT). Resistance to these two antibiotics has dramatically increased in the last years, reaching resistance rates of 27.5% worldwide for CLT^[53] and 94.6% in Bangladesh for MTZ.^[54] Apart from the East and Southeast areas of Asia, even in France, the MTZ-resistance peaked at 58.6%.^[55] Thus, it is highly desirable for new antibacterial agents to be effective on various resistant phenotypes to find a future application in the treatment of current drug-resistant infections. Also, compounds active against the MTZ-resistant ATCC 43504 strain were also tested in combination with MTZ to assess their ability to synergize restoring the susceptibility to MTZ.

2.4.1 | MIC and MBC evaluation of representative thiadiazoles and triazolethiones against *H. pylori* ATCC 43504

Some derivatives (**11b**, **14a**, **17a,b**, **18a**, **19b**, **20a,b**, **24a**, and **25b**) from both series were selected to undergo antibacterial evaluation against *H. pylori* ATCC 43504. Thereby, the minimal inhibitory concentration (MIC) and minimal bactericidal concentration (MBC) of *H. pylori* ATCC 43504 strain were determined via microdilution method, CFU count method, and alamarBlue viability assay by using CLR and MTZ as reference antibiotics (Table 3).

A lack of activity at the maximum concentration tested (128 µg/mL) was observed for most compounds. Interestingly, two derivatives, one from the thiadiazole series (**20a**) and the other from the triazolethiones (**19b**) showed a remarkable antibacterial activity at MIC corresponding to 16 and 8 µg/mL, respectively, while **20b** and **25b** resulted in a weak anti-*H. pylori* activity, with MIC values equal to 128 µg/mL. Notably, **19b** and **20a** also displayed a bactericidal effect at a concentration of 32 µg/mL, whereas MBC values for **20b** and **25b** are identical to their MICs (128 µg/mL) (Table 3). Remarkably, all four active compounds (**19b**, **20a,b**, and **25b**) possessed MIC values improved than those

TABLE 3 MIC and MBC values for selected compounds and reference antibiotics against two *H. pylori* strains.

Cpd	<i>H. pylori</i> ATCC 43504	
	MIC (µg/mL)	MBC (µg/mL)
11b	>128	>128
14a	>128	>128
17a	>128	>128
17b	>128	>128
18a	>128	>128
19b	8	32
20a	16	32
20b	128	128
24a	>128	>128
25b	128	128
AAZ	2048	2048
ETZ	64	128
CLR	0.0078	0.0078
MTZ	16	32

Abbreviations: AAZ, acetazolamide; CLR, clarithromycin; ETZ, ethoxazolamide; MBC, minimal bactericidal concentration; MIC, minimal inhibitory concentration; MTZ, metronidazole.

of the well-known CAs inhibitors AAZ and ethoxazolamide (ETZ) (Table 3).

Then, the two most promising compounds (**19b** and **20a**) were also tested against a clinical isolate, namely *H. pylori* F1, previously identified by Gram-staining and characterized in terms of catalase, urease, and oxidase activity and antibiotic susceptibility with MTZ, CLR, and amoxicillin as benchmarks.^[56] MIC and MBC values on the F1 isolate are reported in Table 4.

Comparable bioactivity emerged on both strains, thus highlighting the molecular target(s) of the compounds maintained in the resistant phenotypes.

TABLE 4 MIC and MBC values for selected compounds **19b** and **20a** and reference antibiotic CLR against *H. pylori* F1 strain.

CPD	<i>H. pylori</i> F1	
	MIC (µg/mL)	MBC (µg/mL)
19b	16	32
20a	16	32
CLR	<0.125	<0.125

Note: MIC and MBC values are expressed as µg/mL and are the mean of experiments performed at least in triplicate using the alamarBlue assay and the colony-forming unit (CFU) count, respectively.

Abbreviations: CLR, clarithromycin; MBC, minimal bactericidal concentration; MIC, minimal inhibitory concentration.

2.4.2 | Antibacterial activity of a combination of **19b** and **20a** with MTZ

Through checkerboard assay, the antibacterial effects in terms of MICs and MBCs of combinations of compounds **19b** and **20a** with MTZ were assessed and the results are reported in Table 5.

Both combinations **19b**+MTZ and **20a**+MTZ showed a decrease in both MIC and MBC values of MTZ compared to the compounds tested individually. Unfortunately, Fractional Inhibitory Concentration (FIC) Indexes (FICIs) were assessed to be equal to 1.125, defining the combinations as indifferent (Table 5). However, Fractional Bactericidal Concentration (FBC) Index (FBCI) was found ≤ 1 , thereby confirming an additive effect for both combinations (Table 5). The decrease in MIC and MBC values of MTZ could be promising in restoring the drug efficacy also against resistant strains.

3 | CONCLUSIONS

In summary, we reported the synthesis of a double large library of coumarin derivatives, including 6- and 7-hydroxycoumarin (**a-b**) isomeric portions and an acylated thiosemicarbazide-derived heterocycle selected between the 1,3,4-thiadiazole and the 1,2,4-triazole-3-thione which were obtained by carrying out the intramolecular cyclization reaction at different pH values. More than 30 compounds (**10–18a,b** and **19–26a,b**) were easily and quickly synthesized and isolated by just filtrating them off from the reaction mixture. Then, they were screened on a wide panel of α - and η - classes of bacterial and protozoan CAs, highlighting specific isoform preference and, in some cases, selectivity towards the isoenzyme belonging to *H. pylori* over the human and the other microbial CAs. Molecular docking simulations of the coumarin derivatives in the closed and open conformations into the HpaCA binding site helped rationalize the different ranges of CA inhibitory activity *in wet* and a relevant interaction network emerged for the most potent compounds. Translating the enzymatic activity to a cellular context led to the antibacterial susceptibility testing on two *H. pylori* strains, the reference ATCC 43504 strain and a

clinical isolate (F1 strain), characterized by different drug-resistant profiles. Compounds **19b** and **20a** showed a moderate anti-*H. pylori* activity and bactericidal effect, along with the ability to reduce the MIC and MBC values of MTZ in combination, even if no synergistic action was detected.

Although already endorsed and validated, herein, we again highlighted the HpaCA enzyme as a valuable pharmacological target in the search for innovative mechanisms of action to be exploited for anti-*H. pylori* agents development. Relevantly, antibacterial susceptibility evaluation on compounds **19b** and **20a** seems to corroborate the idea that this target is not mutated or changed in MTZ-resistant clinical isolate F1, thus laying the foundation for further investigation. In particular, the inhibition of HpaCA by coumarin-containing compounds could be proposed as a valid therapeutic strategy for the development of new anti-*H. pylori* agents or antibiotic adjuvants.

4 | EXPERIMENTAL

4.1 | Chemistry

4.1.1 | General chemistry

Anhydrous solvents and all reagents were purchased from Merck, VWR, and TCI. All reactions involving air- or moisture-sensitive compounds were performed under a nitrogen atmosphere. Nuclear magnetic resonance (^1H and ^{13}C NMR) spectra were recorded using a Bruker Advance III 400 MHz spectrometer in DMSO- d_6 . Chemical shifts are reported in parts per million (ppm) and the coupling constants (J) are expressed in Hertz (Hz). Splitting patterns are designated as follows: s, singlet; d, doublet; t, triplet; m, multiplet; brs, broad singlet. The assignment of exchangeable protons (NH) was confirmed by the addition of D $_2$ O. Analytical thin-layer chromatography (TLC) was carried out on Merck silica gel F-254 plates. Flash chromatography purifications were performed on Merck silica gel 60 (230–400 mesh ASTM) as the stationary phase, and EtOAc and hexane were used as eluents. The solvents used in MS measurements were acetone, ACN (Chromasolv grade), purchased from Sigma-Aldrich (Milan, Italy), and mQ water 18 M Ω , obtained from Millipore's Simplicity system (Milan, Italy). High-resolution mass spectrometry (HRMS) was obtained using a Varian 1200 L triple quadrupole system equipped with an electrospray source (ESI) operating in both positive and negative ions. Stock solutions of analytes were prepared in acetone at 1.0 mg/mL and stored at 4°C. Working solutions of each analyte were freshly prepared by diluting stock solutions in a mixture of mQ H $_2$ O/ACN 1/1 (v/v) up to a concentration of 1.0 µg/mL. The mass spectra of each analyte were acquired by introducing, via a syringe pump at 10 L/min, the working solution. Raw data were collected and processed by Varian Workstation, version 6.8, software.

The InChI codes of the investigated compounds are provided as Supporting Information S2.

TABLE 5 MIC and MBC values for **19b** or **20a** with MTZ in combination with each other and the corresponding FICI and FBICI values, against *H. pylori* ATCC 43504.

<i>H. pylori</i> ATCC 43504	MTZ		19b		20a		FICI ^a	FBICI ^b
	MIC (µg/mL)	MBC (µg/mL)	MIC (µg/mL)	MBC (µg/mL)	MIC (µg/mL)	MBC (µg/mL)		
CPD alone	16	32	8	32	16	32	-	-
Combinations								
19b + MTZ	2	16	8	8	-	-	1.125	0.75
20a + MTZ	2	16	-	-	16	16	1.125	1.0

Note: MIC and MBC values are expressed as µg/mL and are the mean of experiments performed at least in triplicate by means of alamarBlue assay and the colony forming unit (CFU) count, respectively. ^aFICI = (MIC_A^{comb}/MIC_A^{alone}) + (MIC_B^{comb}/MIC_B^{alone}); ^bFBICI = (MBC_A^{comb}/MBC_A^{alone}) + (MBC_B^{comb}/MBC_B^{alone}); ^{a-b}In combinations of A and B, the letters indicate the drugs in the order they appear.

Abbreviations: MBC, minimal bactericidal concentration; MIC, minimal inhibitory concentration; MTZ, metronidazole.

4.1.2 | General procedure for the synthesis of acyl thiosemicarbazides 1–9a,b

Acyl thiosemicarbazides **1–9a,b** were prepared as previously reported.^[35,36]

4.1.3 | General procedure for the synthesis of 10–18a,b

A mixture of the suitable coumarin **1–9ab** (0.05 mmol, 1.0 eq.) and concentrated H₂SO₄ (10 mL) was stirred in an ice bath for 2–3 h till completion. Then, slush was added the formed precipitate was filtered, washed with H₂O and Et₂O, and dried under vacuum.

6-[[5-(Phenylamino)-1,3,4-thiadiazol-2-yl]methoxy]-2H-chromen-2-one (**10a**): 65% yield; m.p. 177–179°C; ¹H NMR (400 MHz, DMSO-*d*₆): 5.50 (2H, s), 6.54 (1H, d, *J* (Hz) = 9.6), 7.41 (2H, m), 7.49 (1H, s), 7.59 (4H, m), 8.04 (1H, d, *J* (Hz) = 9.6), 10.58 (1H, s, exchange with D₂O, NH); ¹³C NMR (100 MHz, DMSO-*d*₆): 65.7, 113.6, 117.7, 118.4, 118.5, 120.1, 121.0, 123.0, 130.0, 141.3, 144.8, 149.4, 154.6, 156.1, 160.9, 166.5; MS (ESI+) *m/z*: 352.0 [M + H]⁺. HRMS (*m/z*) [M + H]⁺: For C₁₈H₁₃N₃O₃S calculated: 352.0751, found: 352.0763.

7-[[5-(Phenylamino)-1,3,4-thiadiazol-2-yl]methoxy]-2H-chromen-2-one (**10b**): 69% yield; m.p. 223–224°C; ¹H NMR (400 MHz, DMSO-*d*₆): 5.57 (2H, s), 6.36 (1H, d, *J* (Hz) = 9.5), 7.05 (1H, t, *J* (Hz) = 7.4), 7.11 (1H, dd, *J* (Hz) = 2.4, 8.6), 7.22 (1H, d, *J* (Hz) = 2.4), 7.38 (2H, m), 7.64 (2H, m), 7.71 (1H, d, *J* (Hz) = 8.6), 8.04 (1H, d, *J* (Hz) = 9.5); ¹³C NMR (100 MHz, DMSO-*d*₆): 65.4, 102.8, 113.6, 113.8, 113.9, 118.4, 122.8, 129.7, 130.2, 141.3, 144.7, 155.2, 155.9, 160.7, 161.2, 166.5; MS (ESI+) *m/z*: 352.0 [M + H]⁺. Experimental data agree with published information.^[33] HRMS (*m/z*) [M + H]⁺: For C₁₈H₁₃N₃O₃S calculated: 352.0751, found: 352.0758.

6-[[5-(*p*-Tolylamino)-1,3,4-thiadiazol-2-yl]methoxy]-2H-chromen-2-one (**11a**): 97% yield; m.p. 200–202°C (dec.); ¹H NMR (400 MHz, DMSO-*d*₆): 2.29 (3H, s), 5.48 (2H, s), 6.54 (1H, d, *J* (Hz) = 9.6), 7.18 (2H, d, *J* (Hz) = 8.5), 7.37 (1H, dd, *J* (Hz) = 2.8, 9.0), 7.42 (1H, d, *J* (Hz) = 9.0), 7.50 (3H, m), 8.04 (1H, d, *J* (Hz) = 9.6); ¹³C NMR (100 MHz, DMSO-*d*₆):

21.2, 65.7, 113.6, 117.7, 118.4, 118.5, 120.2, 121.0, 130.3, 132.1, 139.0, 144.7, 149.3, 154.6, 155.8, 160.9, 166.7, MS (ESI+) *m/z*: 366.0 [M + H]⁺. HRMS (*m/z*) [M + H]⁺: For C₁₉H₁₅N₃O₃S calculated: 366.0907, found: 366.0916.

7-[[5-(*p*-Tolylamino)-1,3,4-thiadiazol-2-yl]methoxy]-2H-chromen-2-one (**11b**): 74% yield; m.p. 225–227°C; ¹H NMR (400 MHz, DMSO-*d*₆): 2.29 (3H, s), 5.56 (2H, s), 6.36 (1H, d, *J* (Hz) = 9.5), 7.10 (1H, dd, *J* (Hz) = 2.4, 8.6), 7.19 (3H, m), 7.52 (2H, d, *J* (Hz) = 8.4), 7.70 (1H, d, *J* (Hz) = 8.6), 8.04 (1H, d, *J* (Hz) = 9.5); ¹³C NMR (100 MHz, DMSO-*d*₆): 21.2, 65.4, 102.9, 113.8, 113.9, 114.0, 118.5, 130.3, 130.5, 132.0, 138.9, 145.0, 155.1, 156.1, 161.0, 161.3, 166.8; MS (ESI+) *m/z*: 366.0 [M + H]⁺. HRMS (*m/z*) [M + H]⁺: For C₁₉H₁₅N₃O₃S calculated: 366.0907, found: 366.0923.

6-[[5-[[4-Chlorophenyl]amino]-1,3,4-thiadiazol-2-yl]methoxy]-2H-chromen-2-one (**12a**): 83% yield; m.p. 241–243°C (dec.); ¹H NMR (400 MHz, DMSO-*d*₆): 5.51 (2H, s), 6.54 (1H, d, *J* (Hz) = 9.6), 7.37 (1H, dd, *J* (Hz) = 2.8, 9.0), 7.43 (3H, m), 7.48 (1H, d, *J* (Hz) = 2.8), 7.69 (2H, d, *J* (Hz) = 8.9), 8.04 (1H, d, *J* (Hz) = 9.6), 10.62 (1H, s, exchange with D₂O, NH); ¹³C NMR (100 MHz, DMSO-*d*₆): 65.6, 113.6, 117.7, 118.4, 119.9, 120.1, 120.9, 126.3, 129.8, 140.2, 144.7, 149.3, 154.5, 156.6, 160.9, 166.0; MS (ESI-) *m/z*: 383.9 [M-H]⁻. HRMS (*m/z*) [M + H]⁺: For C₁₈H₁₂ClN₃O₃S calculated: 386.0361, found: 386.0370.

7-[[5-[[4-Chlorophenyl]amino]-1,3,4-thiadiazol-2-yl]methoxy]-2H-chromen-2-one (**12b**): 84% yield; m.p. 222–224°C; ¹H NMR (400 MHz, DMSO-*d*₆): 5.58 (2H, s), 6.36 (1H, d, *J* (Hz) = 9.5), 7.10 (1H, dd, *J* (Hz) = 8.6, 2.3), 7.22 (1H, d, *J* (Hz) = 2.3), 7.43 (2H, d, *J* (Hz) = 8.9), 7.70 (3H, m), 8.04 (1H, d, *J* (Hz) = 9.5), 10.63 (1H, s, exchange with D₂O, NH); ¹³C NMR (100 MHz, DMSO-*d*₆): 65.4, 102.9, 113.8, 114.0, 119.9, 126.4, 129.8, 130.5, 140.2, 145.0, 156.0, 156.1, 161.0, 161.3, 166.2; MS (ESI+) *m/z*: 385.9 [M + H]⁺. HRMS (*m/z*) [M + H]⁺: For C₁₈H₁₂ClN₃O₃S calculated: 386.0361, found: 386.0367.

6-[[5-[[4-Fluorophenyl]amino]-1,3,4-thiadiazol-2-yl]methoxy]-2H-chromen-2-one (**13a**): 80% yield; m.p. 211–213°C (dec.); ¹H NMR (400 MHz, DMSO-*d*₆): 5.49 (2H, s), 6.54 (1H, d, *J* (Hz) = 9.6), 7.22 (2H, t, *J* (Hz) = 8.8), 7.40 (2H, m), 7.48 (1H, s), 7.67 (2H, m), 8.04 (1H, d, *J* (Hz) = 9.6), 10.50 (1H, s, exchange with D₂O, NH); ¹³C NMR (100 MHz, DMSO-*d*₆): 65.7, 113.6, 116.6 (d, ²*J* (Hz) = 23), 117.8, 118.4, 120.2

(d, 3J (Hz) = 8), 120.2, 121.0, 137.9 (d, 4J (Hz) = 2), 144.8, 149.3, 154.6, 156.1, 158.2, 160.9, 166.5; ^{19}F NMR (376 MHz, DMSO- d_6): -121.0 (1F, s); MS (ESI+) m/z : 369.9 [M + H] $^+$. HRMS (m/z) [M + H] $^+$: For $\text{C}_{18}\text{H}_{12}\text{FN}_3\text{O}_3\text{S}$ calculated: 370.0656, found: 370.0664.

7-([5-[(4-Fluorophenyl)amino]-1,3,4-thiadiazol-2-yl]methoxy)-2H-chromen-2-one (**13b**): 75% yield; 202–204°C (dec.); ^1H NMR (400 MHz, DMSO- d_6): 5.57 (2H, s), 6.36 (1H, d, J (Hz) = 9.5), 7.10 (1H, m), 7.22 (3H, m), 7.68 (3H, m), 8.04 (1H, d, J (Hz) = 9.5); ^{13}C NMR (100 MHz, DMSO- d_6): 65.4, 102.9, 113.9, 114.0, 116.5 (d, 2J (Hz) = 22), 120.2 (d, 3J (Hz) = 8), 130.5, 137.8 (d, 4J (Hz) = 2), 145.1, 155.5, 156.0, 158.3 (d, 1J (Hz) = 237), 161.0, 161.3, 166.6; ^{19}F NMR (376 MHz, DMSO- d_6): -120.9 (1F, s); MS (ESI+) m/z : 369.9 [M + H] $^+$. HRMS (m/z) [M + H] $^+$: For $\text{C}_{18}\text{H}_{12}\text{FN}_3\text{O}_3\text{S}$ calculated: 370.0656, found: 370.0660.

6-([5-[(4-Iodophenyl)amino]-1,3,4-thiadiazol-2-yl]methoxy)-2H-chromen-2-one (**14a**): 68% yield; m.p. 240–241°C (dec.); ^1H NMR (400 MHz, DMSO- d_6): 5.51 (2H, s), 6.54 (1H, d, J (Hz) = 9.6), 7.40 (2H, m), 7.49 (3H, m), 7.70 (2H, d, J (Hz) = 8.7), 8.04 (1H, d, J (Hz) = 9.6), 10.60 (1H, s, exchange with D_2O , NH); ^{13}C NMR (100 MHz, DMSO- d_6): 65.7, 85.9, 113.6, 117.7, 118.4, 120.1, 120.6, 121.0, 138.5, 141.1, 144.8, 149.3, 154.5, 156.6, 160.9, 165.9; MS (ESI-) m/z : 475.9 [M - H] $^-$. HRMS (m/z) [M + H] $^+$: For $\text{C}_{18}\text{H}_{12}\text{IN}_3\text{O}_3\text{S}$ calculated: 477.9717, found: 477.9725.

7-([5-[(4-Iodophenyl)amino]-1,3,4-thiadiazol-2-yl]methoxy)-2H-chromen-2-one (**14b**): 85% yield; m.p. 162–164°C (dec.); ^1H NMR (400 MHz, DMSO- d_6): 5.57 (2H, s), 6.36 (1H, d, J (Hz) = 9.5), 7.10 (1H, dd, J (Hz) = 2.3, 8.6), 7.21 (1H, d, J (Hz) = 2.3), 7.51 (2H, d, J (Hz) = 8.6), 7.70 (3H, m), 8.04 (1H, d, J (Hz) = 9.5), 10.60 (1H, exchange with D_2O , NH); ^{13}C NMR (100 MHz, DMSO- d_6): 65.4, 85.4, 102.9, 113.6, 113.8, 113.9, 120.7, 130.3, 138.3, 141.0, 144.7, 155.9, 160.7, 161.1, 166.1; MS (ESI+) m/z : 477.8 [M + H] $^+$. HRMS (m/z) [M + H] $^+$: For $\text{C}_{18}\text{H}_{12}\text{IN}_3\text{O}_3\text{S}$ calculated: 477.9717, found: 477.9729.

6-([5-[(3-Iodophenyl)amino]-1,3,4-thiadiazol-2-yl]methoxy)-2H-chromen-2-one (**15a**): 71% yield; m.p. 191–193°C; ^1H NMR (400 MHz, DMSO- d_6): 5.51 (2H, s), 6.54 (1H, d, J (Hz) = 9.5), 7.17 (1H, t, J (Hz) = 8.0), 7.36–7.44 (3H, m), 7.49 (1H, d, J (Hz) = 2.8), 7.54 (1H, ddd, J (Hz) = 0.9, 2.2, 8.9), 8.04 (1H, d, J (Hz) = 9.5), 8.21 (1H, t, J (Hz) = 1.9); ^{13}C NMR (100 MHz, DMSO- d_6): 65.6, 95.8, 113.6, 117.6, 117.7, 118.4, 120.1, 121.0, 126.4, 131.3, 131.9, 142.5, 144.7, 149.3, 154.5, 156.8, 160.9, 165.9; MS (ESI-) m/z : 475.9 [M - H] $^-$. HRMS (m/z) [M + H] $^+$: For $\text{C}_{18}\text{H}_{12}\text{IN}_3\text{O}_3\text{S}$ calculated: 477.9717, found: 477.9723.

7-([5-[(3-Iodophenyl)amino]-1,3,4-thiadiazol-2-yl]methoxy)-2H-chromen-2-one (**15b**): 89% yield; m.p. 161–163°C; ^1H NMR (400 MHz, DMSO- d_6): 5.59 (2H, s), 6.37 (1H, d, J (Hz) = 9.4), 7.11 (1H, dd, J (Hz) = 2.5, 8.6), 7.18 (1H, t, J (Hz) = 8.0), 7.22 (1H, d, J (Hz) = 2.5), 7.40 (1H, ddd, J (Hz) = 1.0, 1.6, 7.8), 7.55 (1H, ddd, J (Hz) = 1.0, 1.6, 7.8), 7.71 (1H, d, J (Hz) = 8.6), 8.05 (1H, d, J (Hz) = 9.4), 8.20 (1H, t, J (Hz) = 2.0), 10.61 (1H, s, exchange with D_2O , NH); ^{13}C NMR (100 MHz, DMSO- d_6): 65.5, 95.9, 103.0, 113.9, 114.1, 114.1, 117.7, 126.5, 130.6, 131.5, 131.9, 142.5, 145.1, 156.1, 156.3, 161.1, 161.3, 166.1; MS (ESI+) m/z : 477.8 [M + H] $^+$. HRMS (m/z) [M + H] $^+$: For $\text{C}_{18}\text{H}_{12}\text{IN}_3\text{O}_3\text{S}$ calculated: 477.9717, found: 477.9726.

6-([5-[[4-(Trifluoromethyl)phenyl]amino]-1,3,4-thiadiazol-2-yl]methoxy)-2H-chromen-2-one (**16a**): 84% yield; m.p. 210–212°C; ^1H

NMR (400 MHz, DMSO- d_6): 5.53 (2H, s), 6.55 (1H, d, J (Hz) = 9.6), 7.41 (2H, m), 7.50 (1H, s), 7.74 (2H, d, J (Hz) = 8.5), 7.86 (2H, d, J (Hz) = 8.5), 8.05 (1H, d, J (Hz) = 9.6), 10.90 (1H, s, exchange with D_2O , NH); ^{13}C NMR (100 MHz, DMSO- d_6): 65.7, 113.6, 117.8, 118.2, 118.4, 120.2, 121.0, 122.7 (q, 2J (Hz) = 32), 125.4 (q, 1J (Hz) = 269), 127.3 (q, 3J (Hz) = 4.0), 144.5 (q, 4J (Hz) = 1.0), 144.8, 149.4, 154.5, 157.4, 160.9, 165.8; ^{19}F NMR (376 MHz, DMSO- d_6): -60.0 (3F, s); MS (ESI-) m/z : 417.9 [M - H] $^-$. HRMS (m/z) [M + H] $^+$: For $\text{C}_{19}\text{H}_{12}\text{F}_3\text{N}_3\text{O}_3\text{S}$ calculated: 420.0624, found: 420.0630.

7-([5-[[4-(Trifluoromethyl)phenyl]amino]-1,3,4-thiadiazol-2-yl]methoxy)-2H-chromen-2-one (**16b**): 91% yield; m.p. 229–231°C (dec.); ^1H NMR (400 MHz, DMSO- d_6): 5.61 (2H, s), 6.37 (1H, d, J (Hz) = 9.5), 7.11 (1H, dd, J (Hz) = 2.3, 8.6), 7.23 (1H, d, J (Hz) = 2.3), 7.73 (3H, m), 7.86 (2H, m), 8.04 (1H, d, J (Hz) = 9.5), 10.91 (1H, s, exchange with D_2O , NH); ^{13}C NMR (100 MHz, DMSO- d_6): 65.4, 102.9, 113.9, 114.0, 114.0, 118.2, 122.8 (q, 2J (Hz) = 32), 127.3 (q, 3J (Hz) = 3), 128.11 (q, 1J (Hz) = 271), 130.6, 144.5, 145.1, 156.1, 156.8, 161.0, 161.3, 165.9; ^{19}F NMR (376 MHz, DMSO- d_6): -60.0 (3F, s); MS (ESI+) m/z : 419.9 [M + H] $^+$. HRMS (m/z) [M + H] $^+$: For $\text{C}_{19}\text{H}_{12}\text{F}_3\text{N}_3\text{O}_3\text{S}$ calculated: 420.0624, found: 420.0632.

6-([5-[[4-(Methylthio)phenyl]amino]-1,3,4-thiadiazol-2-yl]methoxy)-2H-chromen-2-one (**17a**): 93% yield; m.p. 197–198°C (dec.); ^1H NMR (400 MHz, DMSO- d_6): 2.48 (3H, s), 5.49 (2H, s), 6.54 (1H, d, J (Hz) = 9.5), 7.32 (2H, d, J (Hz) = 8.3), 7.40 (2H, m), 7.48 (1H, s), 7.61 (2H, d, J (Hz) = 8.3), 8.04 (1H, d, J (Hz) = 9.5), 10.49 (1H, s, exchange with D_2O , NH); ^{13}C NMR (100 MHz, DMSO- d_6): 16.7, 65.7, 113.6, 117.7, 118.4, 119.1, 120.1, 121.0, 128.8, 131.2, 139.0, 144.7, 149.3, 154.5, 156.0, 160.9, 166.2; MS (ESI+) m/z : 397.9 [M + H] $^+$. HRMS (m/z) [M + H] $^+$: For $\text{C}_{19}\text{H}_{15}\text{N}_3\text{O}_3\text{S}_2$ calculated: 398.0628, found: 398.0631.

7-([5-[[4-(Methylthio)phenyl]amino]-1,3,4-thiadiazol-2-yl]methoxy)-2H-chromen-2-one (**17b**): 85% yield; m.p. 200–202°C; ^1H NMR (400 MHz, DMSO- d_6): 2.48 (3H, s), 5.57 (2H, s), 6.36 (1H, d, J (Hz) = 9.5), 7.10 (1H, dd, J (Hz) = 2.4, 8.6), 7.22 (1H, d, J (Hz) = 2.4), 7.32 (2H, d, J (Hz) = 8.7), 7.62 (2H, d, J (Hz) = 8.7), 7.71 (1H, d, J (Hz) = 8.6), 8.04 (1H, d, J (Hz) = 9.5), 10.50 (1H, s, exchange with D_2O , NH); ^{13}C NMR (100 MHz, DMSO- d_6): 16.8, 65.4, 102.8, 113.6, 113.8, 113.9, 119.2, 128.8, 130.3, 131.3, 139.0, 144.7, 155.3, 155.9, 160.7, 161.2, 166.4; MS (ESI+) m/z : 397.9 [M + H] $^+$. HRMS (m/z) [M + H] $^+$: For $\text{C}_{19}\text{H}_{15}\text{N}_3\text{O}_3\text{S}_2$ calculated: 398.0628, found: 398.0637.

6-([5-[[3-Nitrophenyl]amino]-1,3,4-thiadiazol-2-yl]methoxy)-2H-chromen-2-one (**18a**): 75% yield; m.p. 228–230°C; ^1H NMR (400 MHz, DMSO- d_6): 5.54 (2H, s), 6.54 (1H, d, J (Hz) = 9.6), 7.40 (2H, m), 7.49 (1H, d, J (Hz) = 2.8), 7.66 (1H, t, J (Hz) = 8.2), 7.89 (2H, m), 8.04 (1H, d, J (Hz) = 9.6), 8.78 (1H, t, J (Hz) = 2.1); ^{13}C NMR (100 MHz, DMSO- d_6): 65.6, 112.2, 113.6, 117.2, 117.7, 118.4, 120.2, 121.0, 124.3, 131.3, 142.2, 144.7, 149.2, 149.3, 154.5, 157.5, 160.9, 165.8; MS (ESI-) m/z : 394.9 [M - H] $^-$. HRMS (m/z) [M + H] $^+$: For $\text{C}_{18}\text{H}_{12}\text{N}_4\text{O}_5\text{S}$ calculated: 397.0601, found: 397.0609.

7-([5-[[3-Nitrophenyl]amino]-1,3,4-thiadiazol-2-yl]methoxy)-2H-chromen-2-one (**18b**): 65% yield; m.p. 215–217°C; ^1H NMR (400 MHz, DMSO- d_6): 5.62 (2H, s), 6.37 (1H, d, J (Hz) = 9.5), 7.12 (1H, dd, J (Hz) = 2.4, 8.6), 7.23 (1H, d, J (Hz) = 2.3), 7.70 (2H, m), 7.91 (2H, m), 8.05 (1H, d, J (Hz) = 9.5), 8.78 (1H, t, J (Hz) = 2.0); ^{13}C NMR (100 MHz,

DMSO- d_6): 65.4, 102.9, 112.3, 113.8, 114.0, 114.1, 117.2, 124.4, 130.5, 131.3, 142.2, 145.0, 149.3, 156.0, 156.9, 161.0, 161.3, 166.0; MS (ESI-) m/z : 394.9 [M - H]⁻. HRMS (m/z) [M + H]⁺: For C₁₈H₁₂N₄O₅S calculated: 397.0601, found: 397.0611.

4.1.4 | General procedure to synthesize coumarins 19–26a,b

The coumarin compound **1-8a,b** (0.51 mmol, 1.0 eq.) was added to 2 M NaOH aqueous solution (4.0 mL) and the reaction mixture was stirred under reflux for 2 h. After cooling, the mixture was acidified with a diluted solution of HCl. The precipitated product was filtered, washed with H₂O and Et₂O, and dried under vacuum.

6-[[4-Phenyl-5-thioxo-4,5-dihydro-1H-1,2,4-triazol-3-yl]methoxy]-2H-chromen-2-one (**19a**): 86% yield; m.p. 245–247°C (dec.); ¹H NMR (400 MHz, DMSO- d_6): 5.06 (2H, s), 6.51 (1H, d, J (Hz) = 9.5), 7.11 (1H, m), 7.22 (1H, m), 7.33 (1H, m), 7.49–7.59 (5H, m), 7.96 (1H, d, J (Hz) = 9.5), 14.11 (1H, s, exchange with D₂O, NH); ¹³C NMR (100 MHz, DMSO- d_6): 61.7, 113.4, 117.6, 118.2, 120.0, 120.8, 128.9, 130.1, 130.4, 134.2, 144.6, 148.7, 149.3, 154.3, 160.8, 169.6; MS (ESI-) m/z : 349.9 [M - H]⁻. HRMS (m/z) [M + H]⁺: For C₁₈H₁₃N₃O₃S calculated: 352.0751, found: 352.0758.

7-[[4-Phenyl-5-thioxo-4,5-dihydro-1H-1,2,4-triazol-3-yl]methoxy]-2H-chromen-2-one (**19b**): 87% yield; m.p. 270–272°C (dec.); ¹H NMR (400 MHz, DMSO- d_6): 5.14 (2H, s), 6.34 (1H, d, J (Hz) = 9.5), 6.85 (1H, dd, J (Hz) = 2.3, 8.6), 7.00 (1H, d, J (Hz) = 2.3), 7.54 (5H, m), 7.62 (1H, d, J (Hz) = 8.6), 7.99 (1H, d, J (Hz) = 9.5), 14.12 (1H, s, exchange with D₂O, NH); ¹³C NMR (100 MHz, DMSO- d_6): 61.4, 102.7, 113.5, 114.0, 128.9, 130.1, 130.3, 130.4, 134.1, 144.9, 148.3, 155.8, 160.8, 160.9, 169.6; MS (ESI+) m/z : 352.0 [M + H]⁺. Experimental information in agreement with reported data.^[33] HRMS (m/z) [M + H]⁺: For C₁₈H₁₃N₃O₃S calculated: 352.0751, found: 352.0761.

6-[[5-Thioxo-4-(p-tolyl)-4,5-dihydro-1H-1,2,4-triazol-3-yl]methoxy]-2H-chromen-2-one (**20a**): 70% yield; m.p. 243–245°C (dec.); ¹H NMR (400 MHz, DMSO- d_6): 2.37 (3H, s), 5.04 (2H, s), 6.52 (1H, d, J (Hz) = 9.6), 7.14 (1H, dd, J (Hz) = 3.0, 9.0), 7.23 (1H, d, J (Hz) = 3.0), 7.34 (5H, m), 7.97 (1H, d, J (Hz) = 9.6); ¹³C NMR (100 MHz, DMSO- d_6): 21.6, 61.6, 113.5, 117.6, 118.2, 119.9, 120.9, 128.6, 130.6, 131.6, 140.1, 144.6, 148.7, 149.3, 154.3, 160.8, 169.6; MS (ESI-) m/z : 363.9 [M - H]⁻. HRMS (m/z) [M + H]⁺: For C₁₉H₁₅N₃O₃S calculated: 366.0907, found: 366.0913.

7-[[5-Thioxo-4-(p-tolyl)-4,5-dihydro-1H-1,2,4-triazol-3-yl]methoxy]-2H-chromen-2-one (**20b**): 65% yield; m.p. 263–265°C (dec.); ¹H NMR (400 MHz, DMSO- d_6): 2.37 (3H, s), 5.12 (2H, s), 6.34 (1H, d, J (Hz) = 9.5), 6.88 (1H, dd, J (Hz) = 2.1, 8.6), 6.99 (1H, d, J (Hz) = 2.1), 7.34 (4H, s), 7.63 (1H, d, J (Hz) = 8.6), 8.00 (1H, d, J (Hz) = 9.5), 14.07 (1H, s, exchange with D₂O, NH); ¹³C NMR (100 MHz, DMSO- d_6): 21.6, 61.4, 102.8, 113.6, 114.0, 114.1, 128.6, 130.3, 130.6, 131.5, 140.1, 144.9, 148.4, 155.8, 160.9, 169.7; MS (ESI+) m/z : 366.0 [M + H]⁺. HRMS (m/z) [M + H]⁺: For C₁₉H₁₅N₃O₃S calculated: 366.0907, found: 366.0918.

6-[[4-(4-Chlorophenyl)-5-thioxo-4,5-dihydro-1H-1,2,4-triazol-3-yl]methoxy]-2H-chromen-2-one (**21a**): 58% yield; m.p. 252–254°C

(dec.); ¹H NMR (400 MHz, DMSO- d_6): 5.09 (2H, s), 6.52 (1H, d, J (Hz) = 9.6), 7.14 (1H, dd, J (Hz) = 2.9, 9.0), 7.24 (1H, d, J (Hz) = 2.9), 7.34 (1H, d, J (Hz) = 9.0), 7.55 (2H, d, J (Hz) = 8.7), 7.64 (2H, d, J (Hz) = 8.7), 7.97 (1H, d, J (Hz) = 9.6), 14.14 (1H, s, exchange with D₂O, NH); ¹³C NMR (100 MHz, DMSO- d_6): 61.7, 113.5, 117.7, 118.2, 120.0, 120.8, 130.2, 130.9, 133.1, 135.1, 144.6, 148.6, 149.3, 154.2, 160.8, 169.6; MS (ESI-) m/z : 383.9 [M - H]⁻. HRMS (m/z) [M + H]⁺: For C₁₈H₁₂ClN₃O₃S calculated: 386.0361, found: 386.0357.

7-[[4-(4-Chlorophenyl)-5-thioxo-4,5-dihydro-1H-1,2,4-triazol-3-yl]methoxy]-2H-chromen-2-one (**21b**): 85% yield; m.p. 246–248°C (dec.); ¹H NMR (400 MHz, DMSO- d_6): 5.18 (2H, s), 6.35 (1H, d, J (Hz) = 9.5), 6.87 (1H, dd, J (Hz) = 2.3, 8.6), 7.01 (1H, d, J (Hz) = 2.3), 7.55 (2H, d, J (Hz) = 8.6), 7.63 (3H, m), 8.00 (1H, d, J (Hz) = 9.5), 14.16 (1H, s, exchange with D₂O, NH); ¹³C NMR (100 MHz, DMSO- d_6): 61.4, 102.8, 113.5, 114.0, 114.1, 130.2, 130.3, 130.9, 133.0, 135.1, 144.9, 148.3, 155.8, 160.8, 160.9, 169.6; MS (ESI+) m/z : 385.9 [M + H]⁺. HRMS (m/z) [M + H]⁺: For C₁₈H₁₂ClN₃O₃S calculated: 386.0361, found: 386.0368.

6-[[4-(4-Fluorophenyl)-5-thioxo-4,5-dihydro-1H-1,2,4-triazol-3-yl]methoxy]-2H-chromen-2-one (**22a**): 65% yield; m.p. 236–238°C (dec.); ¹H NMR (400 MHz, DMSO- d_6): 5.07 (2H, s), 6.52 (1H, d, J (Hz) = 9.5), 7.13 (1H, dd, J (Hz) = 3.0, 9.0), 7.24 (1H, d, J (Hz) = 3.0), 7.34 (1H, d, J (Hz) = 9.0), 7.41 (2H, m), 7.57 (2H, m), 7.97 (1H, d, J (Hz) = 9.5); ¹³C NMR (100 MHz, DMSO- d_6): 61.7, 113.5, 117.1 (d, ² J (Hz) = 23), 117.7, 118.3, 120.0, 120.9, 130.5 (d, ⁴ J (Hz) = 3), 131.4 (d, ³ J (Hz) = 9), 144.7, 148.8, 149.4, 154.2, 160.9, 163.1 (d, ¹ J (Hz) = 245), 169.8; ¹⁹F NMR (376 MHz, DMSO- d_6): -111.6 (1F, s); MS (ESI-) m/z : 367.9 [M - H]⁻. HRMS (m/z) [M + H]⁺: For C₁₈H₁₂FN₃O₃S calculated: 370.0656, found: 370.0667.

7-[[4-(4-Fluorophenyl)-5-thioxo-4,5-dihydro-1H-1,2,4-triazol-3-yl]methoxy]-2H-chromen-2-one (**22b**): 78% yield; m.p. 242–244°C (dec.); ¹H NMR (400 MHz, DMSO- d_6): 5.16 (2H, s), 6.35 (1H, d, J (Hz) = 9.5), 6.87 (1H, dd, J (Hz) = 1.8, 8.6), 7.02 (1H, d, J (Hz) = 1.8), 7.40 (2H, m), 7.56 (2H, m), 7.63 (1H, d, J (Hz) = 8.6), 8.00 (1H, d, J (Hz) = 9.5), 14.13 (1H, s, exchange with D₂O, NH); ¹³C NMR (100 MHz, DMSO- d_6): 61.4, 102.8, 113.5, 114.0, 114.1, 117.1 (d, ² J (Hz) = 23), 130.4, 130.4 (d, ⁴ J (Hz) = 3), 131.4 (d, ³ J (Hz) = 9), 145.0, 148.4, 155.9, 160.9, 160.9, 163.1 (d, ¹ J (Hz) = 245), 169.8; ¹⁹F NMR (376 MHz, DMSO- d_6): -111.6 (1F, s); MS (ESI+) m/z : 369.9 [M + H]⁺. HRMS (m/z) [M + H]⁺: For C₁₈H₁₂FN₃O₃S calculated: 370.0656, found: 370.0671.

6-[[4-(4-Iodophenyl)-5-thioxo-4,5-dihydro-1H-1,2,4-triazol-3-yl]methoxy]-2H-chromen-2-one (**23a**): 96% yield; m.p. 242–244°C (dec.); ¹H NMR (400 MHz, DMSO- d_6): 5.09 (2H, s), 6.53 (1H, d, J (Hz) = 9.6), 7.14 (1H, dd, J (Hz) = 3.0, 9.0), 7.22 (1H, d, J (Hz) = 3.0), 7.32 (3H, m), 7.92 (2H, d, J (Hz) = 8.5), 7.97 (1H, d, J (Hz) = 9.6), 14.13 (1H, s, exchange with D₂O, NH); ¹³C NMR (100 MHz, DMSO- d_6): 61.7, 97.3, 113.5, 117.7, 118.3, 120.0, 120.9, 131.1, 134.1, 139.1, 144.7, 148.6, 149.4, 154.2, 160.9, 169.5; MS (ESI-) m/z : 475.9 [M - H]⁻. HRMS (m/z) [M + H]⁺: For C₁₈H₁₂IN₃O₃S calculated: 477.9717, found: 477.9724.

7-[[4-(4-Iodophenyl)-5-thioxo-4,5-dihydro-1H-1,2,4-triazol-3-yl]methoxy]-2H-chromen-2-one (**23b**): 81% yield; m.p. 244–245°C (dec.); ¹H NMR (400 MHz, DMSO- d_6): 5.17 (2H, s), 6.35 (1H, d, J (Hz) = 9.5), 6.86 (1H, dd, J (Hz) = 1.9, 8.6), 7.00 (1H, s), 7.30 (2H, d, J (Hz) = 8.3), 7.63 (1H, d, J (Hz) = 8.6), 7.91 (2H, d, J (Hz) = 8.3), 8.00 (1H, d, J (Hz) = 9.5), 14.13 (1H, s, exchange with D₂O, NH); ¹³C NMR

(100 MHz, DMSO- d_6): 61.4, 97.2, 102.8, 113.5, 114.1, 114.1, 130.3, 131.1, 134.0, 139.0, 144.9, 148.3, 156.0, 160.8, 160.9, 169.5; MS (ESI+) m/z : 477.8 [M + H]⁺. HRMS (m/z) [M + H]⁺: For C₁₈H₁₂IN₃O₃S calculated: 477.9717, found: 477.9730.

6-([4-(3-Iodophenyl)-5-thioxo-4,5-dihydro-1H-1,2,4-triazol-3-yl]methoxy)-2H-chromen-2-one (**24a**): 69% yield; m.p. 278–280°C (dec.); ¹H NMR (400 MHz, DMSO- d_6): 5.09 (2H, s), 6.52 (1H, d, J (Hz) = 9.6), 7.12 (1H, dd, J (Hz) = 2.9, 8.9), 7.22 (1H, d, J (Hz) = 2.9), 7.35 (2H, m), 7.54 (1H, d, J (Hz) = 7.6), 7.87 (2H, m), 7.96 (1H, d, J (Hz) = 9.6); ¹³C NMR (100 MHz, DMSO- d_6): 61.7, 95.2, 113.5, 117.7, 118.3, 120.0, 120.8, 128.6, 131.9, 135.3, 137.3, 139.1, 144.6, 148.6, 149.4, 154.2, 160.8, 169.5; MS (ESI-) m/z : 475.8 [M - H]⁻. HRMS (m/z) [M + H]⁺: For C₁₈H₁₂IN₃O₃S calculated: 477.9717, found: 477.9727.

7-([4-(3-Iodophenyl)-5-thioxo-4,5-dihydro-1H-1,2,4-triazol-3-yl]methoxy)-2H-chromen-2-one (**24b**): 56% yield; m.p. 135–137°C (dec.); ¹H NMR (400 MHz, DMSO- d_6): 5.17 (2H, s), 6.34 (1H, d, J (Hz) = 9.5), 6.85 (1H, dd, J (Hz) = 1.8, 8.6), 7.00 (1H, d, J (Hz) = 1.8), 7.35 (1H, t, J (Hz) = 7.8), 7.54 (1H, d, J (Hz) = 7.8), 7.63 (1H, d, J (Hz) = 7.8), 7.87 (2H, m), 8.00 (1H, d, J (Hz) = 9.5), 14.12 (1H, s, exchange with D₂O, NH); ¹³C NMR (100 MHz, DMSO- d_6): 61.4, 95.2, 102.8, 113.4, 114.0, 114.1, 128.6, 130.3, 131.9, 135.2, 137.4, 139.1, 144.9, 148.2, 155.8, 160.8, 160.9, 169.6; MS (ESI+) m/z : 477.8 [M + H]⁺. HRMS (m/z) [M + H]⁺: For C₁₈H₁₂IN₃O₃S calculated: 477.9717, found: 477.9729.

6-([5-Thioxo-4-[4-(trifluoromethyl)phenyl]-4,5-dihydro-1H-1,2,4-triazol-3-yl]methoxy)-2H-chromen-2-one (**25a**): 58% yield; m.p. 214–216°C (dec.); ¹H NMR (400 MHz, DMSO- d_6): 5.14 (2H, s), 6.51 (1H, d, J (Hz) = 9.6), 7.08 (1H, dd, J (Hz) = 2.6, 8.9), 7.19 (1H, d, J (Hz) = 2.6), 7.31 (1H, d, J (Hz) = 8.9), 7.78 (2H, m), 7.94 (3H, m), 14.17 (1H, s, exchange with D₂O, NH); ¹³C NMR (100 MHz, DMSO- d_6): 61.8, 113.6, 117.7, 118.2, 119.9, 120.8, 124.6 (q, ¹ J (Hz) = 270.6), 127.3 (q, ³ J (Hz) = 3.2), 130.1, 130.7 (q, ² J (Hz) = 32), 137.9 (q, ⁴ J (Hz) = 1.6), 144.6, 148.5, 149.4, 154.2, 160.8, 169.5; ¹⁹F NMR (376 MHz, DMSO- d_6): -61.2 (3F, s); MS (ESI-) m/z : 417.9 [M - H]⁻. HRMS (m/z) [M + H]⁺: For C₁₉H₁₂F₃N₃O₃S calculated: 420.0624, found: 420.0635.

7-([5-Thioxo-4-[4-(trifluoromethyl)phenyl]-4,5-dihydro-1H-1,2,4-triazol-3-yl]methoxy)-2H-chromen-2-one (**25b**): 54% yield; m.p. 224–226°C (dec.); ¹H NMR (400 MHz, DMSO- d_6): 5.22 (2H, s), 6.34 (1H, d, J (Hz) = 9.4), 6.82 (1H, dd, J (Hz) = 2.0, 8.7), 6.97 (1H, d, J (Hz) = 2.0), 7.60 (1H, d, J (Hz) = 8.7), 7.77 (2H, m), 7.93 (2H, m), 7.99 (1H, d, J (Hz) = 9.4), 14.17 (1H, s, exchange with D₂O, NH); ¹³C NMR (100 MHz, DMSO- d_6): 61.5, 102.8, 113.5, 114.1, 114.1, 124.6 (q, ¹ J (Hz) = 271.1), 127.3 (q, ³ J (Hz) = 3), 130.2, 130.3, 130.7 (q, ² J (Hz) = 33), 137.9, 144.9, 148.3, 155.8, 160.8, 160.9, 169.6; ¹⁹F NMR (376 MHz, DMSO- d_6): -61.2 (3F, s); MS (ESI-) m/z : 417.9 [M - H]⁻. HRMS (m/z) [M + H]⁺: For C₁₉H₁₂F₃N₃O₃S calculated: 420.0624, found: 420.0638.

6-([4-[4-(Methylthio)phenyl]-5-thioxo-4,5-dihydro-1H-1,2,4-triazol-3-yl]methoxy)-2H-chromen-2-one (**26a**): 96% yield; m.p. 224–226°C (dec.); ¹H NMR (400 MHz, DMSO- d_6): 2.51 (3H, s), 5.08 (2H, s), 6.53 (1H, d, J (Hz) = 9.5), 7.17 (1H, dd, J (Hz) = 2.7, 9.0), 7.24 (1H, d, J (Hz) = 2.7), 7.35 (1H, d, J (Hz) = 9.0), 7.42 (4H, m), 7.98 (1H, d, J (Hz) = 9.5), 14.10 (1H, s, exchange with D₂O, NH); ¹³C NMR (100 MHz, DMSO- d_6): 15.2, 61.7, 113.5, 117.7, 118.3, 120.0, 120.9, 126.8, 129.4,

130.7, 141.3, 144.7, 148.8, 149.4, 154.3, 160.9, 169.7; MS (ESI-) m/z : 395.9 [M - H]⁻. HRMS (m/z) [M + H]⁺: For C₁₉H₁₅N₃O₃S₂ calculated: 398.0628, found: 398.0639.

7-([4-[4-(Methylthio)phenyl]-5-thioxo-4,5-dihydro-1H-1,2,4-triazol-3-yl]methoxy)-2H-chromen-2-one (**26b**): 70% yield; m.p. 240–241°C (dec.); ¹H NMR (400 MHz, DMSO- d_6): 2.52 (3H, s), 5.15 (2H, s), 6.34 (1H, d, J (Hz) = 9.5), 6.88 (1H, d, J (Hz) = 8.6), 7.01 (1H, s), 7.40 (4H, m), 7.63 (1H, d, J (Hz) = 8.6), 8.00 (1H, d, J (Hz) = 9.5), 14.12 (1H, s); ¹³C NMR (100 MHz, DMSO- d_6): 15.2, 61.4, 102.8, 113.5, 114.0, 114.1, 126.8, 129.3, 130.3, 130.6, 141.3, 144.9, 148.5, 155.8, 160.9, 169.8; MS (ESI+) m/z : 397.9 [M + H]⁺. HRMS (m/z) [M + H]⁺: For C₁₉H₁₅N₃O₃S₂ calculated: 398.0628, found: 398.0641.

4.2 | In vitro carbonic anhydrase inhibition assays

The CA-catalyzed CO₂ hydration activity was performed on an Applied Photophysics stopped-flow instrument (SX20 stopped-flow spectrometer Applied Photophysics) using Phenol Red, at a concentration of 0.2 mM, as a pH indicator working at the maximum absorbance of 557 nm with 20 mM HEPES (*N*-2-hydroxyethylpiperazine-*N'*-2-ethanesulfonic acid, pH 7.40 for α -CAs and 8.40 for β -CAs and γ -CAs) as the buffer, 20 mM Na₂SO₄ to maintain constant ionic strength, and following the initial rates of the CA-catalyzed CO₂ hydration reaction for a period of 10–100 s and The CO₂ concentrations ranged from 1.7 to 17 mM for the determination of the kinetic parameters and inhibition constants.^[57] Enzyme concentrations ranged between 5 and 12 nM.^[37,42] For each inhibitor, at least six traces of the initial 5%–10% of the reaction have been used to determine the initial velocity. The uncatalyzed reaction rates were determined in the same manner and subtracted from the total observed rates. Stock solutions of inhibitor (0.1 mM) were prepared in distilled-deionized water, and dilutions up to 0.01 nM were prepared. Solutions containing inhibitor and enzyme were preincubated for 18 h at room temperature before performing the assay to allow the formation of the E–I complex. The inhibition constants were obtained by nonlinear least-squares methods using PRISM 3 and the Cheng–Prusoff equation as reported earlier and represent the mean from at least three different determinations. hCAs I and II were purchased, while the other isoforms were recombinant and obtained *in-house*, as reported earlier.^[11,37–42]

4.3 | Molecular docking

Ligands were sketched in 2D with the Picto Application version 4.4.0.4 (OpenEye, Cadence Molecular Sciences)^[58] and converted into 3D structures with the OMEGA Application version 3.1.0.3 (OpenEye, Cadence Molecular Sciences).^[59,60] Ionization of molecules was carried out by the QUACPAC Application version 2.0.0.3 (OpenEye, Cadence Molecular Sciences).^[61] Ligand energy minimization was performed with SZYBKI version 1.10.0.3 (OpenEye, Cadence Molecular Sciences).^[62] The crystallographic

structure of the HpaCA coded by PDB ID: 4XFW^[48] was used as rigid receptors in molecular docking simulations performed with the GOLD program version 2020.1,^[63] using settings refined in previous works.^[50–52,64,65] The catalytic Zn(II) ion was selected as the center of the binding site, having a radius of 10 Å. For each ligand, 10 runs of the genetic algorithm (GA) were performed. The CHEMPLP scoring function with default parameters was used, while the GA search efficiency was increased up to 200%.

4.4 | Antibacterial susceptibility testing

4.4.1 | Bacterial strains and media

H. pylori ATCC 43504 strain was purchased from ATCC (LGC Standards S.r.l.), while *H. pylori* F1 strain is a clinical strain isolated by a patient affected by gastritis provided by Prof. Francesca Sisto from the University of Milan, Italy.^[13] The strains were stored at –80°C and cultivated as previously described.^[9]

4.4.2 | MIC and MBC determination

Antibacterial susceptibility was evaluated in Brain Heart Infusion broth (BHI; Oxoid Limited) plus 5% of fetal bovine serum (FBS; Sigma-Aldrich) by using the broth microdilution method according to the guidelines of the Clinical and Laboratory Standards Institute^[66] with some modifications.^[9] The results obtained were confirmed by using the alamarBlue (AB) (Thermo Fisher Scientific) viability assay as previously described.^[67] Each compound was prepared as 1.42% (v/v) solution in DMSO and was used in the range of 0.0625–128 µg/mL. Controls consisting of (i) *H. pylori* broth cultures in BHI plus 5% of FBS without the addition of the tested molecule; (ii) *H. pylori* broth cultures in BHI plus 5% of FBS plus 1.42% (v/v) of DMSO without the addition of the tested molecules; (iii) *H. pylori* broth cultures tested with clarithromycin, metronidazole or ethoxazolamide (as positive control); (iv) BHI plus 5% of FBS with the tested molecules; (v) just BHI plus 5% of FBS. Three independent experiments were performed in triplicate. The bacterial initial inoculum was 2–8 × 10⁵ CFU/mL. The incubation was carried out at 37°C for 72 h in microaerobic conditions (Campygen, Oxoid Limited). MIC was defined via the alamarBlue assay, as previously described.^[67] Subsequently, given that alamarBlue is nontoxic against bacteria, MBC was determined, starting from the wells stained with alamarBlue: the entire volume present in the blue-purple wells was seeded on the selected agar plates and incubated at 37°C for 5 days in microaerobic conditions.

4.4.3 | Evaluation of synergism via the checkerboard method

The antibacterial activity of the combinations was determined by the checkerboard method and evaluated by using the Fractional

Inhibitory or Bactericidal Concentration (FIC/FBC) index (FICI or FBCI) as previously reported.^[67]

ACKNOWLEDGMENTS

A.G. is grateful to TUBITAK (The Scientific and Technological Research Council of Turkey) for the award of the 2219 International Post Doctoral Research Fellowship Program. This research was partially supported by the Italian Ministry for University and Research (MIUR) grant number FISR2019_04819 BacCAD to S.C., C.C., and C.T.S. and by EU funding within the NextGenerationEU-MUR PNRR Extended Partnership initiative on Emerging Infectious Diseases (Project no. PE00000007, INF-ACT). This article is based upon work from COST Action EURESTOP, CA21145, supported by COST (European Cooperation in Science and Technology) M.M. V.P. and S.C. thank Prof. Francesca Sisto (University of Milan, Italy) for providing *H. pylori* F1. M.M. (University of Siena) wishes to thank the OpenEye Free Academic Licensing Program for providing a free academic license for molecular modeling and chemoinformatics software.

CONFLICT OF INTEREST STATEMENT

The authors declare no conflicts of interest.

DATA AVAILABILITY STATEMENT

The data that support the findings of this study are available from the corresponding author upon reasonable request.

ORCID

Arzu Gumus  <http://orcid.org/0000-0001-6459-7692>

Ilaria D'Agostino  <https://orcid.org/0000-0002-4870-7326>

Valentina Puca  <https://orcid.org/0000-0002-6417-876X>

Simone Carradori  <http://orcid.org/0000-0002-8698-9440>

Luigi Cutarella  <http://orcid.org/0009-0004-9789-8060>

Mattia Mori  <https://orcid.org/0000-0003-2398-1254>

Fabrizio Carta  <http://orcid.org/0000-0002-1141-6146>

Andrea Angeli  <https://orcid.org/0000-0002-1470-7192>

Clemente Capasso  <https://orcid.org/0000-0003-3314-2411>

Claudiu T. Supuran  <https://orcid.org/0000-0003-4262-0323>

REFERENCES

- [1] Y. Li, H. Choi, K. Leung, F. Jiang, D. Y. Graham, W. K. Leung, *Lancet Gastroenterol. Hepatol.* **2023**, *8*, 553.
- [2] H. Ismail, V. D. Marshall, M. Patel, M. Tariq, R. A. Mohammad, *J. Am. Pharm. Assoc.* **2022**, *62*(2003), 834.
- [3] Z. Chen, J. Guo, Y. Jiang, Y. Shao, *Environ. Sci. Eur.* **2021**, *33*, 11.
- [4] T. A. Lobie, A. A. Roba, J. A. Booth, K. I. Kristiansen, A. Aseffa, K. Skarstad, M. Bjørås, *Int. J. Infect. Dis.* **2021**, *111*, 322.
- [5] K. Shioda, D. M. Weinberger, M. Mori, *JAMA Intern. Med.* **2020**, *180*, 1569.
- [6] S. S. Lum, A. E. Browner, B. Palis, H. Nelson, D. Boffa, L. M. Nogueira, V. Hawhee, R. M. McCabe, T. Mullett, E. Wick, *JAMA Surg.* **2023**, *158*, 643.
- [7] WHO Publishes List of Bacteria for Which New Antibiotics are Urgently Needed. Available from: <https://www.who.int/news/item/27-02-2017-who-publishes-list-of-bacteria-for-which-new-antibiotics-are-urgently-needed>. Accessed 17 Oct 2023.

- [8] I. D'Agostino, C. Ardino, G. Poli, F. Sannio, M. Lucidi, F. Poggialini, D. Visaggio, E. Rango, S. Filippi, E. Petricci, P. Visca, L. Botta, J.-D. Docquier, E. Dreassi, *Eur. J. Med. Chem.* **2022**, 231, 114158.
- [9] G. Benito, I. D'Agostino, S. Carradori, M. Fantacuzzi, M. Agamennone, V. Puca, R. Grande, C. Capasso, F. Carta, C. T. Supuran, *Future Med. Chem.* **2023**, 15, 1865.
- [10] C. Campestre, V. De Luca, S. Carradori, R. Grande, V. Carginale, A. Scaloni, C. T. Supuran, C. Capasso, *Front. Microbiol.* **2021**, 12, 629163.
- [11] I. Nishimori, T. Minakuchi, K. Morimoto, S. Sano, S. Onishi, H. Takeuchi, D. Vullo, A. Scozzafava, C. T. Supuran, *J. Med. Chem.* **2006**, 49, 2117.
- [12] S. Morishita, I. Nishimori, T. Minakuchi, S. Onishi, H. Takeuchi, T. Sugiura, D. Vullo, A. Scozzafava, C. T. Supuran, *J. Gastroenterol.* **2008**, 43, 849.
- [13] M. Ronci, S. Del Prete, V. Puca, S. Carradori, V. Carginale, R. Muraro, G. Mincione, A. Aceto, F. Sisto, C. T. Supuran, R. Grande, C. Capasso, *J. Enzyme Inhib. Med. Chem.* **2019**, 34, 189.
- [14] A. Maresca, D. Vullo, A. Scozzafava, C. T. Supuran, *J. Enzyme Inhib. Med. Chem.* **2013**, 28, 388.
- [15] M. M. Rahman, A. Tikhomirova, J. K. Modak, M. L. Hutton, C. T. Supuran, A. Roujeinikova, *Gut Pathog.* **2020**, 12, 20.
- [16] I. Nishimori, T. Minakuchi, T. Kohsaki, S. Onishi, H. Takeuchi, D. Vullo, A. Scozzafava, C. T. Supuran, *Bioorg. Med. Chem. Lett.* **2007**, 17, 3585.
- [17] I. D'Agostino, S. Carradori, in *Metalloenzymes in Metalloenzymes* (Eds: C. T. Supuran, W. A. Donald), Academic Press, **2024**, p. 393.
- [18] B. L. Bernardoni, C. La Motta, S. Carradori, I. D'Agostino, in *The Enzymes* (Ed: C. T. Supuran), Academic Press, **2024**.
- [19] C. T. Supuran, *Expert Opin. Investig. Drugs* **2024**, 33, 1.
- [20] S. Giovannuzzi, C. S. Hewitt, A. Nocentini, C. Capasso, D. P. Flaherty, C. T. Supuran, *J. Enzyme Inhib. Med. Chem.* **2022**, 37, 333.
- [21] A. Maresca, C. Temperini, H. Vu, N. B. Pham, S.-A. Poulsen, A. Scozzafava, R. J. Quinn, C. T. Supuran, *J. Am. Chem. Soc.* **2009**, 131, 3057.
- [22] A. Maresca, C. Temperini, L. Pochet, B. Masereel, A. Scozzafava, C. T. Supuran, *J. Med. Chem.* **2010**, 53, 335.
- [23] Y.-C. Lee, M. P. Dore, D. Y. Graham, *Annu. Rev. Med.* **2022**, 73, 183.
- [24] Q. Sun, C. Yuan, S. Zhou, J. Lu, M. Zeng, X. Cai, H. Song, *Front. Cell. Infect. Microbiol.* **2023**, 13, 1257817.
- [25] L. Liu, M. C. Nahata, *Ann. Pharmacother.* **2023**, 57, 1185.
- [26] P. K. Godavarthy, C. Puli, *Cureus* **2023**, 15, 36041.
- [27] M.-Y. Cui, Z.-Y. Cui, M.-Q. Zhao, M.-J. Zhang, Q.-L. Jiang, J.-J. Wang, L.-G. Lu, Y.-Y. Lu, *BMC Microbiol.* **2022**, 22, 321.
- [28] A. Tabei, R. Ejtemaei, A. Mahboubi, P. Saniee, A. Foroumadi, A. Dehdari, A. Almasirad, *BMC Chem.* **2022**, 16, 38.
- [29] M. Saleh, Y. A. Mostafa, J. Kumari, M. M. Thabet, D. Sriram, M. Kandeel, H. H. M. Abdu-Allah, *RSC Med. Chem.* **2023**, 14, 2714.
- [30] S.-Y. Li, Y. Zhang, Y.-N. Wang, L.-C. Yuan, C.-C. Kong, Z.-P. Xiao, H.-L. Zhu, *Bioorg. Chem.* **2023**, 130, 106275.
- [31] L. Beyria, O. Gourbeyre, S. Salillas, A. Mahía, M. D. Díaz de Villegas, J. A. Aínsa, J. Sancho, A. Bousquet-Mélou, A. A. Ferran, *Microbiol. Spectrum* **2024**, 12, e0262323.
- [32] A. I. Shahin, S. Zaib, S.-O. Zaraei, R. A. Kedia, H. S. Anbar, M. T. Younas, T. H. Al-Tel, G. Khoder, M. I. El-Gamal, *PLoS One* **2023**, 18, e0286684.
- [33] A. A. Al-Amiery, A. Y. Musa, A. A. H. Kadhum, A. B. Mohamad, *Molecules* **2011**, 16, 6833.
- [34] M. Zayane, A. Romdhane, M. Daami-Remadi, H. B. Jannet, *J. Chem. Sci.* **2015**, 127, 1619.
- [35] A. Gumus, M. Bozdog, A. Akdemir, A. Angeli, S. Selleri, F. Carta, C. T. Supuran, *Molecules* **2022**, 27, 4610.
- [36] A. Peperidou, S. Bua, M. Bozdog, D. Hadjipavlou-Litina, C. Supuran, *Molecules* **2018**, 23, 153.
- [37] M. Fantacuzzi, I. D'Agostino, S. Carradori, F. Liguori, F. Carta, M. Agamennone, A. Angeli, F. Sannio, J.-D. Docquier, C. Capasso, C. T. Supuran, *J. Enzyme Inhib. Med. Chem.* **2023**, 38, 2201402.
- [38] C. S. Hewitt, N. S. Abutaleb, A. E. M. Elhassanny, A. Nocentini, X. Cao, D. P. Amos, M. S. Youse, K. J. Holly, A. K. Marapaka, W. An, J. Kaur, A. D. Krabill, A. Elhashif, Y. Elgammal, A. L. Graboski, C. T. Supuran, M. N. Seleem, D. P. Flaherty, *ACS Infect. Dis.* **2021**, 7, 1969.
- [39] D. Vullo, V. De Luca, A. Scozzafava, V. Carginale, M. Rossi, C. T. Supuran, C. Capasso, *Bioorg. Med. Chem. Lett.* **2012**, 22, 7142.
- [40] D. Vullo, V. D. Luca, A. Scozzafava, V. Carginale, M. Rossi, C. T. Supuran, C. Capasso, *Bioorg. Med. Chem.* **2013**, 21, 1534.
- [41] P. Pan, A. B. Vermelho, G. Capaci Rodrigues, A. Scozzafava, M. E. E. Tolvanen, S. Parkkila, C. Capasso, C. T. Supuran, *J. Med. Chem.* **2013**, 56, 1761.
- [42] I. D'Agostino, S. Zara, S. Carradori, V. DeLuca, C. Clemente, C. H. M. Kocken, A.-M. Zeeman, A. Angeli, F. Carta, C. T. Supuran, *ChemMedChem* **2023**, 18, e202300267.
- [43] A. Angeli, M. Pinteala, S. S. Maier, B. C. Simionescu, A. A. Da'dara, P. J. Skelly, C. T. Supuran, *Int. J. Mol. Sci.* **2020**, 21, 1842.
- [44] R. G. Khalifah, *J. Biol. Chem.* **1971**, 246, 2561.
- [45] A. Angeli, M. Pinteala, S. S. Maier, S. Del Prete, C. Capasso, B. C. Simionescu, C. T. Supuran, *J. Enzyme Inhib. Med. Chem.* **2019**, 34, 244.
- [46] A. Angeli, M. Ferraroni, C. T. Supuran, *ACS Med. Chem. Lett.* **2018**, 9, 1035.
- [47] J. K. Modak, Y. C. Liu, C. T. Supuran, A. Roujeinikova, *J. Med. Chem.* **2016**, 59, 11098.
- [48] M. E. Compostella, P. Berto, F. Vallese, G. Zanotti, *Acta Crystallogr. F Struct. Biol. Commun.* **2015**, 71, 1005.
- [49] A. Karioti, F. Carta, C. T. Supuran, *Curr. Pharm. Des.* **2016**, 22, 1570.
- [50] V. Pontecorvi, M. Mori, F. Picarazzi, S. Zara, S. Carradori, A. Cataldi, A. Angeli, E. Berrino, P. Chimenti, A. Ciogli, D. Secci, P. Guglielmi, C. T. Supuran, *Int. J. Mol. Sci.* **2022**, 23, 7950.
- [51] M. Mori, C. T. Supuran, *J. Enzyme Inhib. Med. Chem.* **2022**, 37, 672.
- [52] Y. Cau, D. Vullo, M. Mori, E. Dreassi, C. Supuran, M. Botta, *Molecules* **2018**, 23, 17.
- [53] M. Sholeh, S. Khoshnood, T. Azimi, J. Mohamadi, V. H. Kaviar, M. Hashemian, S. Karamollahi, N. Sadeghifard, H. Heidarzadeh, M. Heidary, M. Saki, *PeerJ* **2023**, 11, e15121.
- [54] H. Aftab, M. Miftahussurur, P. Subsonwong, F. Ahmed, A. A. Khan, Y. Yamaoka, *J. Infect. Dev. Ctries.* **2016**, 10, 245.
- [55] F. Mégraud, C. Alix, P. Charron, L. Bénégat, A. Ducournau, E. Bessède, P. Lehours, *Helicobacter* **2021**, 26, e12767.
- [56] S. Carradori, A. Ammazalorso, S. Niccolai, D. Tanini, I. D'Agostino, F. Melfi, A. Capperucci, R. Grande, F. Sisto, *Pharmaceuticals* **2023**, 16, 1317.
- [57] I. D'Agostino, G. E. Mathew, P. Angelini, R. Venanzoni, G. Angeles Flores, A. Angeli, S. Carradori, B. Marinacci, L. Menghini, M. A. Abdelgawad, M. M. Ghoneim, B. Mathew, C. T. Supuran, *J. Enzyme Inhib. Med. Chem.* **2022**, 37, 986.
- [58] Picto version 4.5.4.1, OpenEye, Cadence Molecular Sciences, Santa Fe, NM. Available from <https://www.eyesopen.com>
- [59] P. C. D. Hawkins, A. G. Skillman, G. L. Warren, B. A. Ellingson, M. T. Stahl, *J. Chem. Inf. Model.* **2010**, 50, 572.
- [60] Omega version 34.2.0.1, OpenEye, Cadence Molecular Sciences. Available from <https://www.eyesopen.com/omega>
- [61] Quacpac version 2.0.0.3, OpenEye, Cadence Molecular Sciences. Available from <http://www.eyesopen.com>
- [62] SZYBKl version 2.5.0.1, OpenEye, Cadence Molecular Sciences. Available from <https://www.eyesopen.com>
- [63] G. Jones, P. Willett, R. C. Glen, A. R. Leach, R. Taylor, *J. Mol. Biol.* **1997**, 267, 727.

- [64] E. Berrino, S. Bua, M. Mori, M. Botta, V. S. Murthy, V. Vijayakumar, Y. Tamboli, G. Bartolucci, A. Mugelli, E. Cerbai, C. T. Supuran, F. Carta, *Molecules* **2017**, *22*, 1049.
- [65] M. Mori, Y. Cau, G. Vignaroli, I. Laurenzana, A. Caivano, D. Vullo, C. T. Supuran, M. Botta, *ACS Chem. Biol.* **2015**, *10*, 1964.
- [66] Clinical and Laboratory Standard Institute, *Performance Standards for Antimicrobial Susceptibility Testing. Seventeenth Informational Supplement M100-S17*, Clinical and Laboratory Standard Institute, Wayne, PA **2007**.
- [67] V. Puca, G. Turacchio, B. Marinacci, C. T. Supuran, C. Capasso, P. Di Giovanni, I. D'Agostino, S. Carradori, R. Grande, *Int. J. Mol. Sci.* **2023**, *24*, 4455.

SUPPORTING INFORMATION

Additional supporting information can be found online in the Supporting Information section at the end of this article.

How to cite this article: A. Gumus, I. D'Agostino, V. Puca, V. Crocetta, S. Carradori, L. Cutarella, M. Mori, F. Carta, A. Angeli, C. Capasso, C. T. Supuran, *Arch. Pharm.* **2024**, e2400548. <https://doi.org/10.1002/ardp.202400548>